

We are IntechOpen, the world's leading publisher of Open Access books Built by scientists, for scientists

6,900

Open access books available

186,000

International authors and editors

200M

Downloads

Our authors are among the

154

Countries delivered to

TOP 1%

most cited scientists

12.2%

Contributors from top 500 universities



WEB OF SCIENCE™

Selection of our books indexed in the Book Citation Index
in Web of Science™ Core Collection (BKCI)

Interested in publishing with us?
Contact book.department@intechopen.com

Numbers displayed above are based on latest data collected.
For more information visit www.intechopen.com



Composite Materials Infiltrated by Aluminium Alloys Based on Porous Skeletons from Alumina, Mullite and Titanium Produced by Powder Metallurgy Techniques

Leszek A. Dobrzański , Grzegorz Matula ,
Anna D. Dobrzańska-Danikiewicz , Piotr Malara ,
Marek Kremzer , Błażej Tomiczek ,
Magdalena Kujawa , Eugeniusz Hajduczek ,
Anna Ahtelik-Franczak , Lech B. Dobrzański and
Jagoda Krzysteczko

Additional information is available at the end of the chapter

<http://dx.doi.org/10.5772/65377>

Abstract

The infiltration technology with reinforcement in the form of porous skeletons fabricated with powder metallurgy methods has been presented in relation to the general characteristics of metal alloy matrix composite materials. The results of our own investigations are presented pertaining to four alternative technologies of fabrication of porous, sintered skeletons, and their structure and their key technological properties are presented. Porous skeletons made of Al_2O_3 aluminium are sintered reactively using blowing agents or are manufactured by ceramic injection moulding (CIM) from powder. Porous skeletons made of $3\text{Al}_2\text{O}_3 \cdot 2\text{SiO}_2$ mullite are achieved by sintering a mixture of halloysite nanotubes together with agents forming an open structure of pores. Titanium porous skeletons are achieved by selective laser sintering (SLS). The structure and properties of composite materials with an aluminium alloy matrix—mainly EN AC- AlSi12 and also EN AC- AlSi7Mg0.3 alloys—reinforced with the so manufactured skeletons are also described. A unique structure of the achieved composite materials, together with good mechanical properties and abrasive wear resistance at low density, ensured by an aluminium alloy matrix, are indicating broad application possibilities of such composites.

Keywords: composite materials, powder metallurgy, infiltration, sintering, SLS, CIM

1. General characteristics of metallic matrix composite materials

Composite materials are one of the key groups of engineering materials, and although their fabrication is often inspired by examples originating from nature, they are produced—by the rule—artificially. They consist of at least two different constituent components with the same or similar volume fraction and with a clearly marked separation boundary between them and with their properties differing from the components creating them. Such properties are principally—for strictly specified reasons—more beneficial than the properties of each of the components, which justifies the need to manufacture them [1–4].

The principal components of a composite material are a matrix and reinforcement, with each of them playing different roles. The majority of composites are manufactured by indirect methods based on the earlier and separate preparation of the matrix and reinforcement materials and then combining them into the whole. A composite material matrix is comprised of a material being the continuous phase, filling the space between the reinforcement, and thus allowing to maintain the matrix-reinforcement system in the compact form, and also ensuring the desired shape and dimensions of products made of such materials. A matrix is also transferring loads onto the reinforcement, and at the same time, it protecting against damages or negative environmental impact, and most frequently, it is also crucial for chemical and thermal properties of the composite material. A matrix material can be either metal, including ferrous alloys, magnesium alloys, aluminium alloys, zinc alloys, silver alloys, nickel alloys and copper alloys. It can also be made of non-metal—a ceramic matrix (aluminium oxide, silicon carbide, aluminium nitride, graphite, cement, chamotte) and an organic matrix: polymeric (e.g. polypropylene, polycarbonate, polyesters, epoxide, polyamide) or a carbon matrix [1–5]. Another component is introduced into a matrix—reinforcement, having better properties, usually strength properties, than the matrix properties. Reinforcement can be either in the form of fibres, particles or elements with complex geometric characteristics and even such ordered spatially, for example, in the form of a skeleton, and its role in a composite is generally to ensure, among others, the required rigidity, increased yield strength and strength at room temperature, to prevent the propagation of cracks and to change matrix susceptibility to plastic deformations [1–5]. Reinforcement is a general term, however, and for this reason, for some composite materials, its role is not only, and in some cases, at all, to improve mechanical or tribological properties, but also to improve selected physicochemical properties, for example, electric, thermal or magnetic properties.

Apart from the properties of the matrix and the reinforcement, the connection between the matrix and the reinforcement, produced as a result of the technology applied, plays an important role in all composite materials. A contact zone between the matrix and the reinforcement is an organic layer in composite materials, whose thickness and physicochemical character are essential for the transfer of loads between the matrix and reinforcement, hence for the properties of the composite material produced [6–10]. Several types of matrix-reinforcement connections can be distinguished considering the character of interactions between the composite material components:

- chemical connections, connected with diffusive processes occurring between a matrix and reinforcement of a composite material and for this reason also often called a diffusive connection;
- mechanical connections, where reinforcement elements are mechanically 'anchored' within the matrix;
- adhesive connections, due to the bonds existing between the adjoining matrix and reinforcement surfaces, often accompanying a mechanical interaction and increasing its effectiveness.

The key factor critical to fabrication of the required connection between a matrix and reinforcement is its surface quality; for this reason, an important part of the technological process of composite material fabrication is to prepare the matrix and reinforcement correctly. A properly selected combination of all or some of the following operations has to be applied most frequently for such preparation, in relation to the matrix and reinforcement, or at least one of them, depending on the composite material manufacturing technology applied [1–4]:

- machining,
- ultrasonic treatment,
- alkaline degreasing,
- degreasing in organic solvents,
- chemical etching,
- electrochemical etching.

One of the composite material variants is a group with a metallic matrix, often called metal matrix composites (MMCs) [1, 2, 4]. Unfaltering interest has been seen in composite materials with a light metal matrix, linked to an effort to minimise the weight of parts used in the automotive, aviation, railway and ship industry to reduce the overall mass of vehicles and by means of transport in which they are incorporated, which, naturally, allows to reduce the mass and improve the coverage and bearing capacity of vehicles while lowering fuel consumption. Hence, more attention is paid to replacing steel parts with relatively high weight with light metal alloys, especially aluminium and magnesium. Unfortunately, a lower Young's modulus, lower strength, tribological properties and rigidity of light metal alloys—as compared to steel—do not always allow to use them as a conventionally manufactured alloy, even subjected to heat treatment. As a consequence, composite materials with a light metal alloy matrix having better strength properties, rigidity, wear resistance, hardness and a lower thermal expansion coefficient are often fabricated in order to improve the mentioned properties [11]. Special attention should be drawn to light metal matrix composite materials reinforced with ceramic particles or ceramic fibres, which—due to very good properties as compared to conventional alloys—such as smaller density, higher strength and creeping resistance and abrasive strength and corrosion resistance, are commonly employed in the aviation, electronic, motor and machine industry, and also in the space and arms sector, and even a sports sector. The technologies of their manufacturing processes are one of

the most sharply evolving fields of materials engineering. In order to address the expectations of the market, it is substantiated to undertake measures aimed at developing alternative methods of light metal matrix composites, mainly aluminium and magnesium alloys [12–22]. Considering a high melting point, low density and good corrosion resistance of ceramics, the fibre-reinforced or particle-reinforced composites deriving from such ceramics are of special importance here. Of special importance, here is also a quest for alternative materials for the commonly used reinforcements in the form of Al_2O_3 fibres and particles [10, 15, 23–25], SiC [6, 13], made of boron [26], whiskers of Al_2O_3 or SiC, B_4C [27], BN [12] and TiC [6, 28] particles, graphene [5] or carbon nanotubes, as well as intermetallic phases [29], and even of high-melting metals and their alloys [30, 31]. In the case of aluminium alloy matrix composites, the name of the matrix element is often provided directly in the name or abbreviation of such a composite, for example, aluminium matrix composites (AlMCs). The considerations presented further in this chapter concern such composite materials.

2. General characteristics of the infiltration technology for the fabrication of metal matrix composite materials with indirect use of powder metallurgy method

Metallic composite materials can be manufactured by various methods. The ones used most often include classical powder metallurgy methods applied directly, as well as mechanical alloying methods and hot and cold plastic consolidation described in detail in other chapters of this book. It is beneficial to fabricate composite materials with powder metallurgy methods due to the diffusive form of the matrix and reinforcement connection, as well as due to flexible choice of the reinforcement type, form and dimensions. Such methods allow to achieve composite materials through the consolidation of metal powders and ceramics, as a result of several successive operations, that is, powder and powder mixture preparation, moulding or compression, sintering or plastic consolidation and finishing. Despite many advantages of such a method, including undoubtedly a possibility to produce a series of elements with high accuracy, a possibility of automating the production and assembly of the elements produced, low power consumption and almost completely eliminated waste production, powder metallurgy requires to use specialist equipment. Moreover, powder production causes difficulties, and it is costly. The mechanical properties of the materials achieved in this way are sometimes worse than, for example, of plastically worked elements. However, owing to mechanical synthesis (mechanical milling) and the subsequent compression and hot pressing, nanostructured composite materials can be manufactured having the constant cross section, uniformly distributed reinforcement and reinforcement particles, and the resulting enhanced mechanical properties of materials [32, 33].

An alternative solution for this technology is a hybrid combination of powder metallurgy methods with a casting technology such as infiltration. In this technology, a porous skeleton with open pores is produced, usually a ceramic skeleton, but in some cases, it is also made of

metals or metal alloys, with powder metallurgy methods. Next, the pores are filled with liquid metal or alloy with a melting point correspondingly lower than the melting point of the metal from which the sintered skeleton was made. Melted polymeric material or special resin mixed with a hardener is also often used for filling. The task of a sintered porous skeleton, being a semi-product, is to finally reinforce, locally, the composite material produced, at the same time determining its structure and properties. The basic property of this porous skeleton, which is also representing the reinforcement of the finally produced composite material, is that it has a structure of open, linked pores forming the channels allowing the melted metal or, respectively, polymeric material to flow freely. As a result of this, a porous preform can be saturated with liquid metal or a polymeric material within the entire volume of pores. This technology can certainly be approached, as it was made in this book, as a special variant of the powder metallurgy technology, but only an indirect one although a description of this technology can also be found in works concerning the casting of metals and metal alloys. In such case, it is usually not mentioned, though, that pores can be filled with polymeric materials in the liquid state, which shows that this technology cannot be classified unequivocally as a metal casting method.

The use of infiltration as a highly profitable technology is fundamental for obtaining a wide array of composite materials and brings numerous technological benefits [23, 25, 34, 35]. This stems from the fact that a technology of fabricating metal matrix composite materials using infiltration is characterised by high efficiency, and it can be utilised in mass production and ensures a wide selection of reinforcement and matrix. Moreover, it entails a smaller risk of mechanical damage to the reinforcement, as can be the case in, for example, mechanical synthesis. Besides, parts can be produced which are reinforced within the whole volume or only locally with the near-net-shape; a structure is also produced having the type of interpenetrating crystalline networks. In view of the characteristics presented, infiltrated composite materials attract manufacturers' special attention, especially in motor industry. Nevertheless, one has to point out the obstacles for applying this technology with the requirement to prepare the internal surfaces of the reinforcement skeleton pores to improve their wettability. It is also necessary to remove the gases absorbed at the surface to avoid gas porosity. Moreover, it is not possible to ensure full reinforcement dispersion in a matrix which is dictated solely by the complex constructional characteristics of the sintered porous skeleton, most often in the form of a porous preform [15, 23, 24, 36].

The infiltration method creates relatively advantageous conditions for recycling the so produced composite materials. It is most preferable for composite materials that they can be re-used in a combined form, that is, without separation of components. Such materials are usually designed for a specifically defined use, and hence, it is difficult to find an area for reusing them. Reinforcement has to be separate from a matrix in such case. This can be done in two ways, mechanically or chemically. In mechanical separation, liquid metal is pressed from a porous skeleton under the acting pressure, or filtration of the liquid matrix is performed. In case of chemical methods of separation, it is necessary to use a material (flux) with a higher affinity from the reinforcing phase than matrix affinity. The material will infiltrate a porous sintered skeleton, by pushing away a matrix from it, which forms, together with it, a composite

material. A material with the lowest solubility in a matrix should be used as a fluxing agent. NaCl-KCl-Na₂SiF₆ used for removing oxide inclusions from a liquid alloy [11] was used for aluminium and its alloys.

A structure and properties of composite materials fabricated by the infiltration of porous sintered skeletons depend on multiple factors, including surface tension and viscosity of liquid metal and infiltration conditions, that is: pressure, addition rate, temperature of sintered skeleton, liquid metal and a moulding for infiltration [37]. The characteristics of a porous skeleton are important, including its porosity, material it is made of, shape and shape of pores, manufacturing method, and such aspect is discussed in detail in the next sub-chapter. Having in mind the multitude of the quantified factors, multi-criteria optimisation is required, and the entire technological process has to be examined thoroughly in order to achieve the required structure and properties of the composite material manufactured by the method of infiltration. For instance, if the temperature of a porous skeleton is lower than a melting point of the infiltrating alloy, it is being partly solidified during infiltration, which is leading to decreased skeleton permeability and makes it difficult to penetrate the porous skeleton by the infiltrating alloy [38, 39].

Depending on the triggering factor and on the required infiltrating pressure of liquid metal or polymeric material, infiltration methods are grouped into three main categories [40, 41]:

- assisted with external pressure;
 - pressure/squeeze infiltration, in which metal—being under the pressure of several dozen or several hundred of MPa—is flowing in and solidifies in skeleton pores under the influence of the gas situated over the metal level (gas infiltration) [6, 40, 42, 43], through a pressing piston of a mould placed in a press (squeeze casting) [13, 35, 38, 39, 44–46], by the activity of centrifugal forces or by applying an electromagnetic field inducing the Lorentz force;
 - low-pressure infiltration in which a pressure of several to several hundreds of Pa is exerted on the gas situated underneath the liquid metal level with a variant of pressureless infiltration where a skeleton is penetrated by liquid metal caused by hydrostatic pressure [27, 28, 43, 47];
- subpressure assisted;
 - vacuum infiltration where a sintered skeleton is placed in the conditions of gas pressure reduced versus atmospheric pressure, and a factor causing infiltration is a positive pressure of the liquid metal [48];
- pressureless infiltration;
 - infiltration assisted by capillary pressure or pressureless infiltration [28, 49, 50] under the activity of hydrostatic pressure.

Gas-pressure infiltration is a combination of vacuum infiltration—because a sintered porous skeleton, before being introduced into liquid metal, stays in the conditions of reduced pressure—and of pressure infiltration as pressure is exerted on the gas, inert gas by the rule, situated under the liquid metal level. This is undoubtedly most advantageous type of

infiltration in technological terms because, during the process, the porous skeleton being sintered as well as the alloy used for its penetration is in a protective atmosphere, that is, in vacuum during alloy melting and in an atmosphere of inert gas after introducing the skeleton into liquid metal. Moreover, vacuum-assisted infiltration allows to reduce a pressure exerted on liquid metal, as its actual pressure should be referred to the vacuum created earlier, not to atmospheric pressure, as in case of conventional pressure infiltration. This is very important due to the fact that alloy pressure cannot exceed a limit value determined by a ceramic skeleton's strength. A significant advantage of the gas-pressure method is low porosity of the final composite material. By applying external pressure, composite materials are achieved with the shape requiring no finishing; it also ensures thorough penetration of a porous skeleton by liquid metal, protecting the product against the occurrence of internal micro-shrinkages being structure discontinuities, thus impacting negatively the composite material produced and deteriorating its strength properties.

The wetting of solid bodies by liquid metal plays an important role in technological processes of composite material manufacturing with a liquid matrix [9, 51]. The following factors are predominant for the wettability of the solid body-liquid configuration [52]:

- the work of adhesion which should be performed to separate the unit surface of the contacting bodies and to create two new surfaces with the value which is a measure of molecular attraction between two different phases and
- the work of cohesion which should be performed to separate the unit surface of the same body and to create two new surfaces with the value which is a measure of molecular attraction between the particles of the same phase.

A characteristic used most often for the degree of wetting of ceramics or metals and their alloys by liquid metal is the wetting angle value θ in the range of 0° (complete wettability) to 180° (complete lack of wettability), which is an important indicator necessary to analyse the phenomena taking place at the solid body/liquid interface. Conventionally, liquid metal-ceramics systems or metals and their alloys in the solid state were grouped into wettable systems, where $\theta < 90^\circ$, and non-wettable systems, where $\theta > 90^\circ$. Different factors may influence the value of θ angle in case where a liquid alloy, for example, Al, is influencing a ceramic or metallic skeleton, for example, Al_2O_3 . The factors are dependent upon the liquid infiltrating metal and include contact time and the presence of an oxide coating on a metal droplet. This factor—in case of aluminium—is the most important factor essential for wettability, and it is dependent, among others, on the atmosphere in which flushing takes place, being a barrier inhibiting the formation of sufficiently good contact of metal with the substrate and increasing the value of θ angle [6–9, 53]. Other factors discussed in another sub-chapter, such as surface roughness, substrate porosity, impurities, relate to a porous skeleton mainly. If the skeleton being wetted is well wetted by liquid metal, infiltration may occur by itself, without being forced externally. Low wettability of the skeleton being sintered or lack thereof is seen in the majority of liquid metal-ceramics interface or metal or metal alloy configurations, as a result of which liquid metal has to be introduced into pores under pressure. Alloy pressure must not, however, exceed the limit value dictated by a sintered skeleton's strength. For this

reason, wettability has to be very often improved before infiltration [6, 38, 42, 43], by decreasing the θ angle value by means of one of the most popular methods [47, 54], applicable to the properties of the liquid infiltrating component, by:

- increasing liquid metal or infiltrating alloy temperature,
- changing the chemical composition of the liquid metal or infiltrating alloy,
- applying a protective atmosphere preventing the oxidisation of metal droplets or infiltrating alloy.

Changes to the chemical composition of liquid metal or infiltrating alloy result from the introduction of alloy additions therein, such as Si, Ti, Mg, Ni, Cr, Ca, Li, which influence surface tension, adhesion work and wetting angle. They additionally cause chemical reactions, mainly in the area of a liquid metal-porous skeleton separation boundary, which may influence the formation of new phases [53]. For example, silicon, as an alloying element in aluminium alloys, is considerably improving the strength of connection; for this reason, an AlSi11/Al₂O₃ connection is better for each temperature as compared to an Al/Al₂O₃ connection, which confirms the suitability of using this alloy as an infiltrating material. Wettability in infiltration is also closely dependent on the properties of the sintered skeleton, which is presented in detail in the next chapter.

3. General characteristics of the structure and properties of porous skeletons manufactured by powder metallurgy methods for infiltration with metal alloys

The basis for composite materials produced by the method of infiltration is porous sintered skeletons produced by powder metallurgy methods, principally determining the structure and properties of the final product. A correctly produced sintered skeleton should be characterised by a structure of open, connected pores, enabling the easiest possible flow of liquid metal. The existence of closed pores or blind channels leads to the occurrence of areas not saturated by the infiltrating metal or alloy. The modern methods of producing porous sintered skeletons can be classified in the following way [25, 34, 35, 38, 44–46, 55, 56]:

- the sintering of ceramic or metallic powders with the addition of, or more rarely, without a binder, as the simplest and most common method in which uncompressed ceramic or metallic powders are sintered, permitting to produce skeletons with porosity of up to 50% or to sinter a mixture of powder grains with a binder added or not, initially pressed under small pressure or to represent a sponge structure;
- the fabrication of metallic or ceramic foam from an appropriately selected mixture, and the method consists of using the released gases as a result of a chemical reaction or decomposition reaction occurring at high temperature, for example:



(Tab) enabling to produce skeletons with porosity of up to 90%;

- the freezing and sublimation of a solvent (usually distilled water) from ceramic or metallic powder suspensions, with a porous structure formed by the volume fraction of the solvent in a suspension, by the rate of freezing and sublimation of, for example, ice under a reduced pressure or gelling the foamed suspension [57];
- the sintering or reactive bonding of ceramic fibres or the sintering of ceramic and metallic powders with an agent added forming the structure of pores. This method is most flexible for all the methods presented here and allows to achieve infiltrated materials with a diverse structure and fraction of the material forming the foamed skeleton. The level of porosity and its character can be controlled by means of different pore-forming agents (PFA) undergoing decomposition at a high temperature, in the place of which voids are created. The most frequently used foaming substances are materials or substances with their thermal decomposition temperature much lower than sintering temperature, such as: polyethylene, wax, starch, celluloses, carbon fibres, sawdust [23, 46, 56]. The principle of this method is the same as the Powder Injection Moulding method and its variant, Ceramic Injection Moulding [58–61], however, a network of open channels has to be created in the sintered matrix after removing a binder and other foaming elements, for example, carbon fibres. This method allows to produce porous semi-products with a diverse structure and fraction of reinforcement and with open, interlinked pores supportive to the thorough penetration of liquid metal in the whole volume of material during infiltration. An agent forming the structure of pores (its fraction being dependent on the planned porosity obtained after removing it from a moulding) is added to ceramic powder (dry or in form of suspension) before pressing to undergo thermal decomposition at an elevated temperature (in a sintering operation).

A fabrication technology of porous sintered skeletons by sintering mineral nanotubes extracted from halloysite – with carbon fibres added as a foaming agent, later subjected to gas-pressure infiltration, was developed under own works [14, 16, 17, 19–22, 62, 63], and the technology is subject to patent protection [49, 50].

The own works [30, 31, 64–66] also highlight that – for this purpose – skeletons can be used of microporous metals and their alloys, also ceramic ones, with the pore size of several dozens to several hundreds of μm , made by the selecting sintering/laser melting SLS/SLM method, which are also covered by patent protection [67–70].

Permeability is the basic factor characterising the structure of open pores and porous channels of sintered skeletons. In permeability examinations, a series of measurements is carried out of the volumetric flow intensity and pressure drop of air, liquid or another factor during transition through a specimen [41]. The important factors determining this property include, in particular, diameter, grain size distribution, shape and volume fraction of the particles/reinforced fibres used [37].

Wettability in infiltration is also dependent on the properties of the sintered reinforcing skeleton. The wettability of porous sintered skeletons is dictated by the chemical composition of the reinforcing material, especially its surface roughness, although it can be assumed that if $R_a < 10$ nm, then the impact of roughness on the wetting angle is irrelevant. It is also dictated by skeleton porosity, because porosity above 5–8% of volume is reducing the wetting angle associated with the penetration of liquid metal inside the pores, and the volume of droplets, being fundamental for measuring the θ wetting angle, is reduced as a result of infiltration. Wettability can only be improved by changing technological conditions of infiltration, but especially by the surface treatment of internal pores of the sintered skeleton. A more and more widespread method of enhancing the wettability of skeletons sintered before infiltration is the deposition of thin layers, mainly metallic layers, onto an inner surface of pores. Such coatings increase a solid body's surface energy γ_c (reinforcing component) and also secure the internal surfaces of pores against damage during production, and inhibit undesired reactions with a liquid infiltrating component, which is important for skeletons made of materials susceptible to oxidisation, such as, graphite or carbon fibres [71, 72].

The special coatings fulfilling such a function are, notably, nickel alloy Ni-P layers, mainly owing to good anticorrosive properties of nickel and its resistance to high temperature, and also its simple deposition technology [10, 15, 23, 24, 48, 51]. Ni-P coatings can be used either by galvanic means, or with a commonly used electroless (chemical, catalytic) method [51, 73]. The electroless deposition method of nickel allows to metal plate practically each material after prior activation of its surface to create active centres needed to initiate the reduction of Ni^{2+} ions. Surface is activated most often using palladium chloride. The reaction is performed further autocatalytically, Ni atoms placed on active centres are becoming a catalyst. The type of the metals deposited is a constraint for this method—only metals from the copper, iron and platinum groups of the periodic table of elements. The more rarely used methods of coating deposition onto sintered skeletons before infiltration include physical and chemical vapour deposition (PVD) and (CVD) and TiO_2 deposition [9, 71–74].

The following chapters of the book present in detail, according to the results of the investigations, four examples of composite materials, infiltrated mainly with eutectic aluminium alloy EN AC- AlSi12 , differing in reinforcing materials. Different skeletons with different chemical and phase composition were produced by different powder metallurgy methods.

The structures of porous skeletons Al_2O_3 were achieved in two ways: In the first method, by mixing Al_2O_3 powder with a pore-forming agent in the form of carbon fibres, the semi-products achieved are characterised by the varied porosity of 68–81% depending on the foaming agent applied. Infiltration was achieved by pressing uniaxially a porous ceramic skeleton and a liquid aluminium alloy into a closed die. In the other case, ceramic injection moulding (CIM) was used for Al_2O_3 ceramic powders by successive injection moulding, binder degradation and sintering using a binder which is a mixture of thermoplastic materials, for example, polypropylene (PP) or polyethylene (PE) with high-melting paraffin and stearic acid, by mixing ceramic powder with a binder using a screw extruding press after heating to the binder plasticisation temperature over the time allowing for the thorough homogenisation of the polymer-powder mixture, by moulding the produced powder-binder slip by injection into a

three-part mould and by the thermal or chemical removal of the binding component followed by sintering. Composite materials can be further fabricated as previously or by gas-pressure infiltration, as in other cases.

Another example concerns a unique technology of fabrication of porous skeletons of reinforcement by the dry mechanical milling of a mixture of halloysite nanotubes with carbon fibres, and of a slipping agent, in the form of powdered amide, micronised in a centrifugal ball mill. Next, a mixture of powders is moulded by uniaxial pressing in dies on a platen hydraulic press under the pressure of 50–100 MPa. The moulded parts are sintered in a high-temperature oven in the atmosphere of air with slow heating to degrade carbon fibres. Heating then takes place at 800°C, which is helping to degrade carbon fibres in the whole volume of specimens, with heating to a sintering temperature and sintering by cooling. Composite materials were produced by gas-pressure infiltration with an eutectic aluminium alloy EN AC- AlSi12 .

A porous skeleton was made in the last of the analysed examples using pristine titanium with micropores dimensioned 100–200 μm by selective laser sintering with an additive method. A 3-D skeleton model was designed by the CAD method using unit cells with a specific structure and size and then by duplicating such a unit cell in order to design a skeleton with a repeatable structure in which the size of pores and wall thickness are fully controlled by the designer, characterised by fully open pores with the porosity of 50–80%. Next, a porous skeleton was produced from titanium powder by sintering it selectively, layer by layer, using an YFL fibre laser with an active material doped with Ytterbium and the maximum power of 200 W in the atmosphere of argon. SLS technique was employed to produce titanium skeletons, which were then used for infiltration with EN AC- AlSi12 alloy.

The following sub-chapters also describe, apart from the mentioned technology of producing porous sintered skeletons, the structure and properties of composite materials fabricated using such skeletons.

4. Structure and properties of porous Al_2O_3 skeletons sintered or manufactured by ceramic injection moulding from powder and of aluminium alloy matrix composite materials reinforced with them

An assumption is underlying the technological works presented in this sub-chapter stating that the application of infiltration allows to achieve multiple benefits while satisfying designers' specific requirements for the manufactured composite materials having a matrix of eutectic aluminium EN AC- AlSi12 alloy, and to a high extent, it is dependent on the construction and technology of a porous skeleton, ceramic Al_2O_3 in this case. It was taken into account that apart from shape selection and selection of the phase fraction, chemical wetting with nickel is influencing the formation of mechanical properties and abrasive wear resistance and corrosion of such materials fabricated by a newly developed method of pressure infiltration of porous sintered Al_2O_3 skeletons constituting a reinforcing phase.

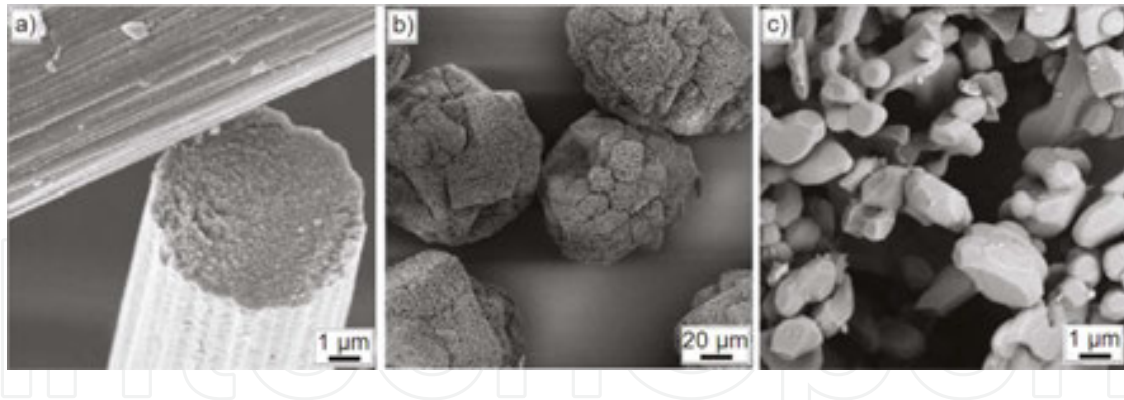


Figure 1. Structure of: (a) carbon fibres of Sigrafil C10 M250 UNS by SGL Carbon Group, (b) Al₂O₃ Alcoa CL 2500 powder as supplied, (c) Al₂O₃ Alcoa CL 2500 powder after milling.

Porous ceramic structures were fabricated by the method of sintering Al₂O₃ CL 2500 powder, by Alcoa Industrial Chemicals, with an agent added forming the structure of pores and channels in the form of carbon fibres, Sigrafil C10 M250 UNS, manufactured by SGL Carbon Group (**Figure 1**). The fabrication of porous ceramic skeletons included the preparation of powders, pressing and sintering. Al₂O₃ CL 2500 powder was milled wet in a ball mill for 5 min to disintegrate the particles concentrated in agglomerations. An agent, Dolapix CE 64, was added to the Al₂O₃ suspension preventing the formation of clusters of carbon fibres and eliminating their mutual electrostatic interactions. The added carbon fibres accounted for, respectively, 30, 40 and 50% by mass. 1% of polyvinyl alcohol, Moviol 18-8, soluble in water, was added to the mixture to facilitate subsequent pressing. The so-prepared powder was subjected to drying, consisting of freezing and sublimation of water under reduced pressure, and sifting through a screen with 0.25 mm eyes. The powders were wetted with polyvinyl alcohol for activation, packed to foil bags and left for 24 h. The powders were subjected to uniaxial pressing with a manual laboratory press, 'Nelke', equipped with a 30 mm diameter die on a platen hydraulic press, Fontune TP 400, supplied with a rectangular die sized 65 × 46 mm. The pressing pressure was, respectively, 25, 50 and 100 MPa, and its interaction time is 15 s. The moulded parts were sintered in a tubular furnace, Gero, in the atmosphere of air under a flow rate of 20 l/min. The thermal stability of carbon fibres, Sigrafil C10 M250 UNS, used as a pore-forming agent in the ceramic skeletons produced from Al₂O₃ Alcoa CL 2500 powder, was determined based on the results of a thermogravimetric (TGA) analysis. The fibres exhibit thermal stability to 390°C, and after exceeding it, their degradation takes place signified by a mass loss, and an increase in a derivative established for the mass loss. The carbon fibres are oxidised until being completely degraded by reaching the temperature of 692°C, determined with the temperature of overall technical degradation. If higher temperature is applied, up to which slow heating is seen, than the degradation temperature of carbon fibres, and when withstanding the material at such temperature, it is assured that the pore-forming agent is completely degraded and the subsequent fast increase in temperature from the rate of 300°C/h will not cause sudden reactions likely to destroy the ceramic skeleton. The tests results obtained allowed to optimise a sintering programme of ceramic porous skeletons. Sintering consists of slow heating to 800°C at a rate of 20°C/h, withstanding at that temperature

for 10 h for complete thermal degradation of carbon fibres, heating to 1500°C at a rate of 300°C/h, sintering for 2 h and cooling in an oven. It was not decided to apply a higher rate of heating to the thermal stability temperature of carbon fibres of 390°C due to the fact that mouldings contained are also an additive facilitating pressing, such as polyvinyl alcohol (1%) and distilled water triggering its activity (3%), the sudden evacuation of which during fast heating could cause skeleton cracks. The skeletons made by pressing a mixture of powders under the pressure of 25 and 50 MPa were characterised by insufficient strength and could crack in further treatment; hence, focus was placed solely on the sintered pressed skeletons under the pressure of 100 MPa.

Commercial semi-products produced were also used for further investigations to compare the properties of composites reinforced with skeletons made of Al₂O₃ particles with materials reinforced with skeletons consisting of fibres. Such semi-products were fabricated by sintering short, cut Al₂O₃ fibres with the diameter of 2–4 µm using a binder in form of silica. The skeletons have a 25% fraction of ceramic phase.

Economic considerations had the main influence on the use of Al₂O₃ powder, as it is about 50 times cheaper than the commonly used Al₂O₃ fibres. Carbon fibres were used as a PFA for technological benefits—their degradation product is CO₂ only, which ensures high process purity and the fact that the matrix material will assume an advantageous, in terms of mechanical properties, shape of degraded carbon fibres. Tar is exuded in case of, for example, wooden fibres or celluloses, which remains as an impurity in the material or settles on the oven walls. Two basic types of pores exist (**Figure 2**), the first of which, with larger size, are formed by degradation of carbon fibres; while the other, smaller ones occur around single ceramic particles and exist because they were not compacted deliberately. No clusters of pores formed after the degraded carbon fibres occur.

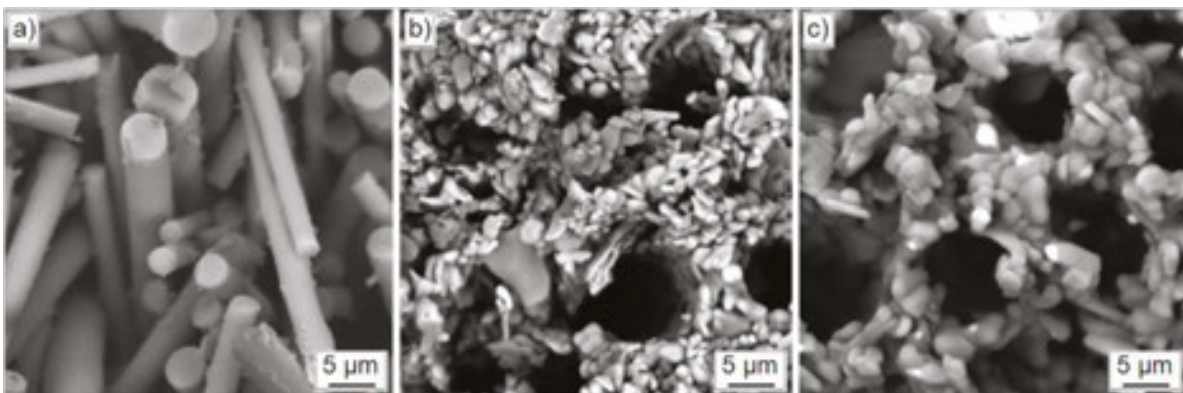


Figure 2. Structure of ceramic skeleton fracture: (a) commercial skeleton produced from Al₂O₃ fibres, (b) produced by sintering Al₂O₃ powder with 30% fraction of carbon fibres, (c) produced by sintering Al₂O₃ powder with 50% fraction of carbon fibres.

The pores and channels of ceramic skeletons were coated with nickel to improve the wettability of Al₂O₃ by a liquid aluminium alloy. Futuron technology by Atotech, used for fabrication of metallic coatings on polymer, was employed to activate the surface of ceramics. A layer of zinc

and palladium was formed on the surface after performing futuron activation. Novigant Activator AK II solution was used to replace zinc on the surface of ceramics with metallic palladium. A layer of Ni-P alloy was deposited onto the so-prepared substrate by the electroless chemical method. The inner parts of the ceramic skeletons could be coated by using a specially constructed device for pumping solutions through them. A spiral coil, made of copper, with a stream of water flowing through it, was mounted on the apparatus to ensure the required temperature of solutions during the deposition of coatings. The skeletons, to prevent their damage during assembly in a device, were glued with a double-component 'UHU plus endfest 300' glue for aluminium rings. The nickel-coated semi-products were then cut out from rings along the glue-ceramics boundary.

The ceramic skeletons produced from Al_2O_3 Alcoa CL 2005 powder and the semi-products composed of Al_2O_3 fibres after a nickel-plating process, and those not nickel-plated, were subjected to infiltration with a liquid EN AC- AlSi12 alloy. The so-prepared ceramic skeletons were heated in an oven to the temperature of 800°C . A sintered ceramic skeleton and a liquid EN AC- AlSi12 alloy with the temperature of 800°C were put inside a mould, covered with graphite, with the temperature of 450°C . All this was covered with a die and placed on a platen hydraulic press, Fontune TP 400. The pressing rate was 17 mm/s, and the maximum press pressure was 100 MPa. The load was removed after 120 s, and the materials removed from the mould were cooled with a stream of compressed air.

Metallographic examinations of the produced composite materials reinforced with the created skeletons achieved by sintering Al_2O_3 particles allowed to confirm the uniform distribution of a reinforcing phase in the matrix (**Figure 3a**). The carbon fibres used as a pore-forming additive during uniaxial pressing of skeletons are oriented perpendicular to the direction of the load applied. In case of powder consolidation by uniaxial pressing, the foaming agent applied, whose one dimension differs largely from others (e.g. fibres, plates), may lead to the occurrence of anisotropy of the created material's properties.

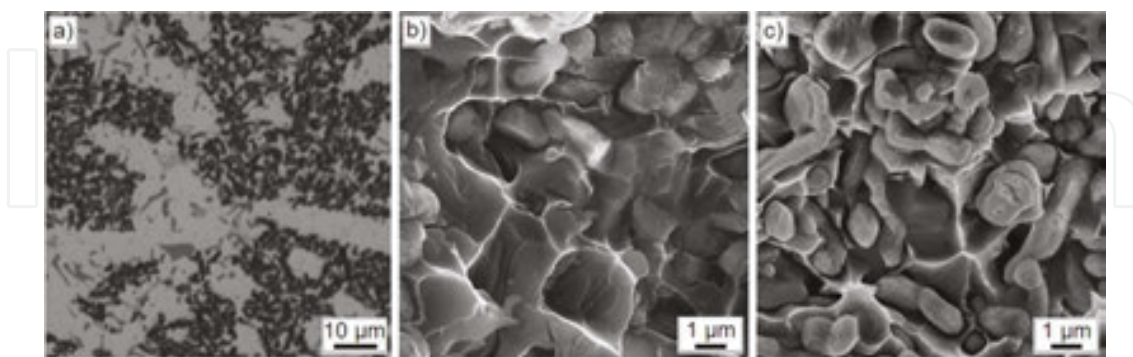


Figure 3. The structure of the created composite material with EN AC- AlSi12 matrix reinforced with porous Al_2O_3 skeleton with 30% fraction of pores: (a) microsection on the plane perpendicular to the pressing direction of porous sintered skeleton, (b) fracture, (c) fracture with pores covered with nickel.

The composite materials created are characterised by advantageous, uniform distribution of the ceramic phase in an aluminium matrix (**Figure 3a**). It was also found that infiltration

takes place completely, as signified by the lack of voids not saturated with metal—even the micropores created on the interface of Al_2O_3 particles are tightly filled under the pressure acting during infiltration. The fracture is of mixed nature; a plastically deformed matrix is around the reinforcing phase, whereas the fracture on the metal-ceramics interface is brittle (**Figure 3b, c**). The presence of numerous Al_2O_3 grains in the structure of such materials was confirmed diffractionally as a result of the examinations (**Figure 4**). A metal matrix, being an Al-based solid solution, and Si grains, making up an eutectic structure of EN AC- AlSi12 alloy, are situated between the regions of Al_2O_3 . The presence of an Ni-based solid solution was also found in the composite materials with an Ni-P coating deposited onto Al_2O_3 . Al_3Ni phase precipitates were identified in the materials with an Ni-P coating deposited onto Al_2O_3 , in the area of the Al-based solid solution (**Figure 5**).

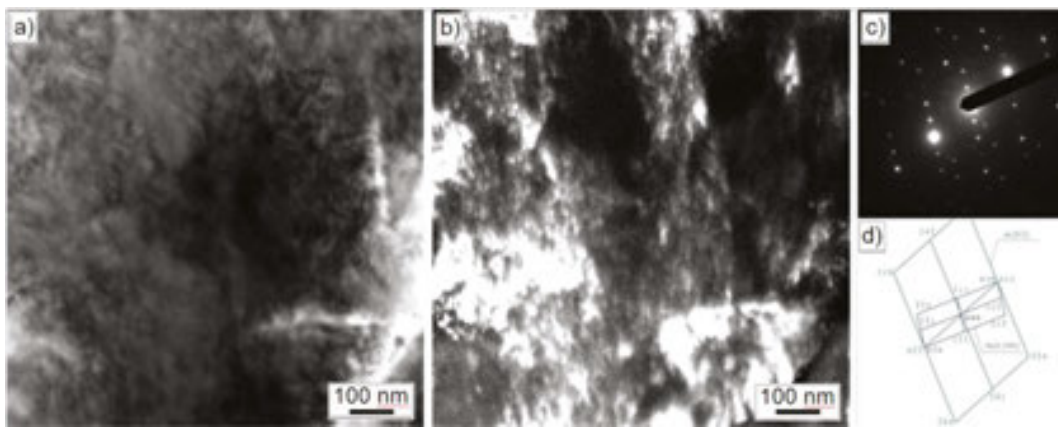


Figure 4. Structure of thin foil made from composite material with EN AC- AlSi12 matrix reinforced with porous Al_2O_3 skeleton with 50% fraction of pores in the porous skeleton: (a) image in bright field, (b) image in the dark field from reflex $1\bar{1}\bar{1}$ Al_2O_3 , (c) diffraction pattern from the area as in **Figure a**, (d) diffraction pattern solution from **Figure c**.

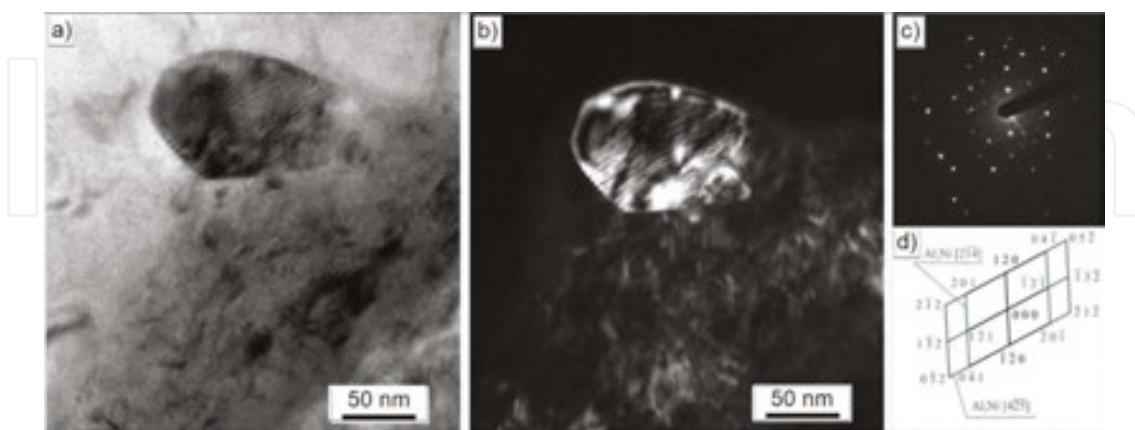


Figure 5. Structure of thin foil made from composite material with EN AC- AlSi12 matrix reinforced with porous Al_2O_3 skeleton coated with Ni with 50% fraction of pores in the porous skeleton: (a) image in bright field, (b) image in the dark field from reflex $\bar{1}\bar{2}0$ Al_3Ni , (c) diffraction pattern from the area as in **Figure a**, (d) diffraction pattern solution from **Figure c**.

The materials fabricated are characterised by hardness higher over two times (43–51 HRA depending on the fraction of a reinforcing phase) as compared to their matrix made up of EN AC- AlSi12 (19 HRA) alloy. The hardness of such materials is rising as the fraction of a ceramic phase is rising.

The reinforcement of an aluminium alloy with porous Al_2O_3 skeletons has a beneficial effect also on the mechanical properties of the materials created. EN AC- AlSi12 alloys have the tensile strength of up to 200 MPa, whereas the maximum tensile strength is seen for the composite materials reinforced with ceramic skeletons produced from particles with a ~25% fraction of Al_2O_3 . Tensile strength is decreasing if a fraction of a ceramic phase is continued to be increased.

If hard reinforcing particles in a soft aluminium alloy matrix are added, this leads to enhanced abrasive wear resistance. The abrasive wear of composite materials is rising as the fraction of a ceramic phase is rising. It was confirmed in the tribological examinations carried out that composite materials feature much smaller wear than their matrix, and the lowest wear is exhibited by a material with the largest fraction of a ceramic phase; moreover, their wear is inversely proportional to the fraction of a ceramic phase regardless the load and the friction path.

The established method of manufacturing a composite material with a matrix made of EN AC- AlSi12 alloy reinforced with porous ceramic skeletons obtained from Al_2O_3 particles, in which they are subjected to pressure infiltration with a liquid aluminium alloy, ensures the required structure and mechanical properties, and also wear resistance much more advantageous as compared to the input aluminium alloy. Composite materials reinforced with the newly developed sintered ceramic skeletons represent, beyond doubts, a cheaper alternative for the extensively used materials reinforced with fibrous semi-products.

This sub-chapter also analysing a technology alternative with regard to the previously discussed method of the successive Al_2O_3 powder consolidations by uniaxial pressing and sintering consisting of ceramic injection moulding (CIM). As a sintered Al_2O_3 porous skeleton is obtained as a result of such activities, the same as previously, the concept of wettability inside the pores of this skeleton as well as the structure and final properties of the obtained composites infiltrated with an aluminium alloy was not analysed again in this case. It was assumed that – despite clear differences in the geometric characteristics of porous skeletons obtained with the two methods, the differences in the properties of composite materials obtained using porous skeletons by each of the methods are irrelevant. The results of examinations for the finally achieved composite materials, which are already presented in the previous sub-chapter for this type of a porous skeleton material, were not repeated, then.

The modern methods of producing porous materials which can be used, in particular, for pressure infiltration, include Powder Injection Moulding, with its variant, metal injection moulding (MIM), where a slip is basically formed with metal powders, or ceramic injection moulding (CIM), where ceramic powders are formed. This is a technique covering the fabrication of products from powders using injection moulding, binder degradation and sintering. This technique allows to obtain products with complicated shapes, with high-quality and strictly defined chemical composition. Injection moulding stands out from other technol-

gies because it requires no finishing, for example, by machining or plastic working, and hence, no problems occur with production of waste such as riser heads, flashes, chips, and the material is used nearly in 100%.

The CIM technology uses ceramic powders, including aluminium oxide powder (Al_2O_3), titanium oxide powder (TiO_2), zirconium oxide powder (ZrO_2) or others. Due to unique properties of ceramic materials, that is, good mechanical properties, small own mass, high resistance and good chemical resistance, they are an interesting material with a broad range of applications in various industries.

A binder has to be used to mould elements by CIM. The main component of the binder is usually a thermoplastic polymeric material, for example, polypropylene (PP) or polyethylene (PE). The injection moulding of ceramic powders is taking place usually in four main steps by mixing ceramic powder with a binder, moulding the slip obtained by injection, by removing the binder and sintering.

Binder component	Density (g/cm^3)	Melting point ($^\circ\text{C}$)	Degradation temperature ($^\circ\text{C}$)
PP	0.89	163	250–450
HDPE	0.94	130	378–500
SA	0.94	73	200–350
PW	0.91	58.3	250–342

Table 1. Overview of example of multi-component binder.

In ceramic injection moulding, ceramic powder is mixed in the first place with a binder which can be a mixture of many binding agents. A technologically optimum binder should have low viscosity in moulding conditions, good wettability of the powder used, chemical or thermal degradability and should be cheap and environment friendly. A powder-to-binder ratio is linked to the powder particle shape, size, powder wettability by a binder and the properties of the binder itself as well as to the slip production conditions. The binder is usually a multi-component binding system (**Table 1**). Thermoplastic polymer materials, such as PP or PE, form a base which, when the binder is removed, is degraded as the last, and they maintain the element's shape at high temperatures. Another binding component reduces slip viscosity and is removed in the first steps of degradation, leaving the pores open, owing to which gas products formed during polymer decomposition can escape freely outside, without causing defects in the material, for example, distortion. For example, high-melting paraffin satisfies such conditions. Another element is a surfactant, for example, stearic acid, whose task is to improve ceramic powder wettability and to improve powder dispersion in a binder, and hence, a homogenous slip of powder with a binder can be produced. An additional task of stearic acid is to lower slip viscosity.

Powder is mixed with a binder using a screw extruding press, where ceramic powder with a binder is heated to the binder plasticisation temperature in time allowing for the thorough homogenisation of the polymer-powder slip. The time needed to homogenise the slip can be set by measuring the torque (**Figure 6**).

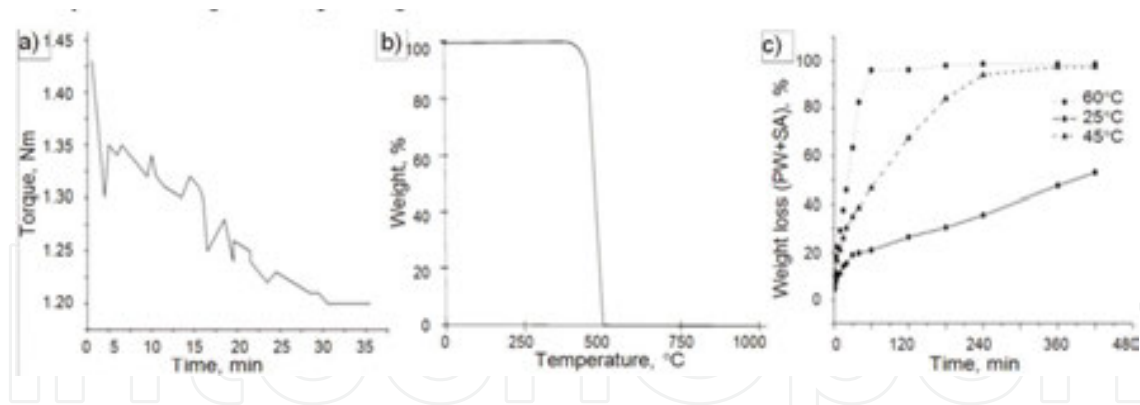


Figure 6. (a) Torque curve for powder-binder slip; (b) TGA result for polyethylene; heating rate of 7.5°C/min to temperature of 1000°C in air; (c) binder degradation by solvating at different temperature, using heptane C_7H_{16} .

A difficulty in preparing the slip is to achieve the homogenous decomposition of powder in a binder. Slip is prepared in an extruder by disintegrating ceramic powder agglomerates to achieve single particles ensuring better dispersion in the slip. Single powder particles have a larger specific surface area, and hence, it is necessary to use a binder with larger fraction to improve ceramic powder wettability. **Table 2** presents the examples of composition of the powder-binder slip.

Feedstocks	Alumina		PP		HDPE		PW		SA	
	%wt	%vol	%wt	%vol	%wt	%vol	%wt	%vol	%wt	%wt
A	50	81.20	22	8.11	0	0	22	8.34	6	2.35
B	50	88.37	0	0	22	9.32	22	9.07	6	2.56
C	50	84.55	11	4.32	11	4.53	22	8.68	6	2.45

Table 2. Examples of composition of powder-binder slip.

Depending on the thermal properties of the powder-binder slip, the extrusion temperature should be higher than the highest melting point of the binder component, but lower than the lowest degradation temperature of each of binder components. A thermogravimetric analysis (TGA) has to be undertaken in order to identify degradation temperature for particular binder components. TGA is a technique of examining the thermal decomposition of materials by examining changes in the mass of the given substance depending on changes in temperature or time.

Another stage in CIM technology is to mould the produced powder-binder slip by injection into a three-part mould, which allows to remove the element produced easier. Problems with extracting an item from a die are caused by low shrinkage of the material produced after injection into a die. Injection temperature and pressure, ensuring the complete filling of the die socket with the material, have to be taken into account to optimise injection. Injection temperature is selected according to the injection temperature selection principle. Insufficient injection temperature may cause problems with injecting the material into a die, whilst

excessive temperature may start degradation of the binder components, which leads releasing the gas created in degradation, thus to bubbles being formed in the item, which are an undesired effect.

Another stage in the process of manufacturing porous sintered skeletons for pressure infiltration is to remove thermally or chemically a binding component with the lowest degradation temperature to open the pores within the whole volume of the item, which enables to quickly remove thermally another binder component with a higher temperature of degradation. If thermal degradation is only used, it begins from the surface and goes inside the material as the temperature is rising. Channels are formed as pores are opening through which gas of the degraded binder with lower degradation temperature is escaping, and thus, pores are further opened allowing to release gas products of the binder component from the deeper and deeper parts of the material. The size of the pores formed due to degradation depends on the size of the powder grain. Thermal degradation is slow because the channels being formed make the path—covered by the gas products escaping—longer than the item thickness. If higher temperature and a higher heating rate are applied, this may lead to specimen deformations or damages—distortion. **Table 3** shows the examples of binder degradation process conditions.

Thermal debinding (steps)	Heating rate (°C/min)	Debinding temperature (°C)	Debinding time (min)
1	3	200	60
2	1	250	30
3	1	300	30
4	1	350	60
5	1	400	60
6	1	450	60
7	1	550	30

Table 3. Binder degradation steps by thermal method.

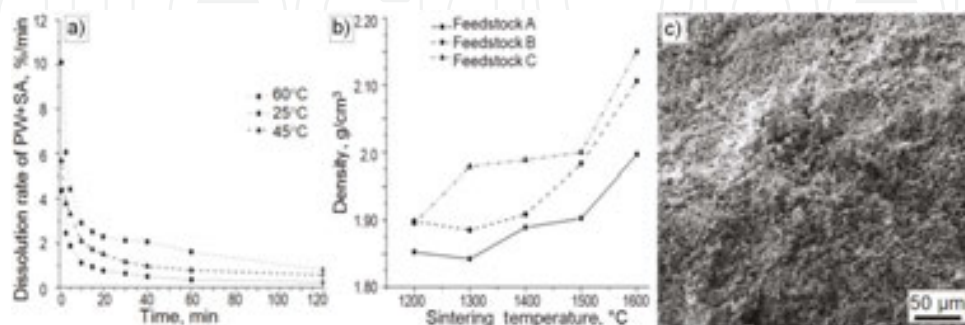


Figure 7. (a) Influence of degradation time and temperature on degradation rate of paraffin and stearic acid; (b) influence of sintering temperature on density of the item produced; (c) structure of porous ceramic skeleton of Al_2O_3 sintered at 1400°C for 1 h (SEM).

Thermal degradation is an alternative to chemical degradation, so-called solvent degradation. Its key benefit is the rate of solving, and a disadvantage is that aggressive and environment unfriendly reagents are used. The solvent method causes smaller element degradations and damages compared to thermal degradation but requires two operations connected with material transition between the initial degradation and extraction of the polymer base by thermal degradation. Chemical degradation combined with thermal degradation is becoming more and more popular. Binder degradation with a solvent is used most often in the first step of degradation of a binder component with the lowest temperature of degradation (**Figure 7**).

Sintering is the last step of a technological process in the production of ceramic porous skeletons decisive for density, porosity and mechanical properties of the ready product. A suitable degradation temperature of particular binder components, and also an oven heating rate, has to be selected based on the data acquired with a TGA analysis. An important factor during sintering is also to select the appropriate atmosphere of filling an oven chamber as it has to enable/assist the degradation process of binder components. All the factors mentioned have an effect on the quality of a ready element.

A higher sintering temperature causes better compaction and smaller porosity by diffusion and also the formation of necks between the sintered powder particles. The effect is reverse in a lower temperature, and skeleton density is decreasing, whilst the porosity is growing.

5. The structure and properties of sintered porous skeletons from mullite obtained by sintering a mixture of halloysite nanotubes with agents forming an open structure of pores and of aluminium alloy matrix composite materials reinforced with it

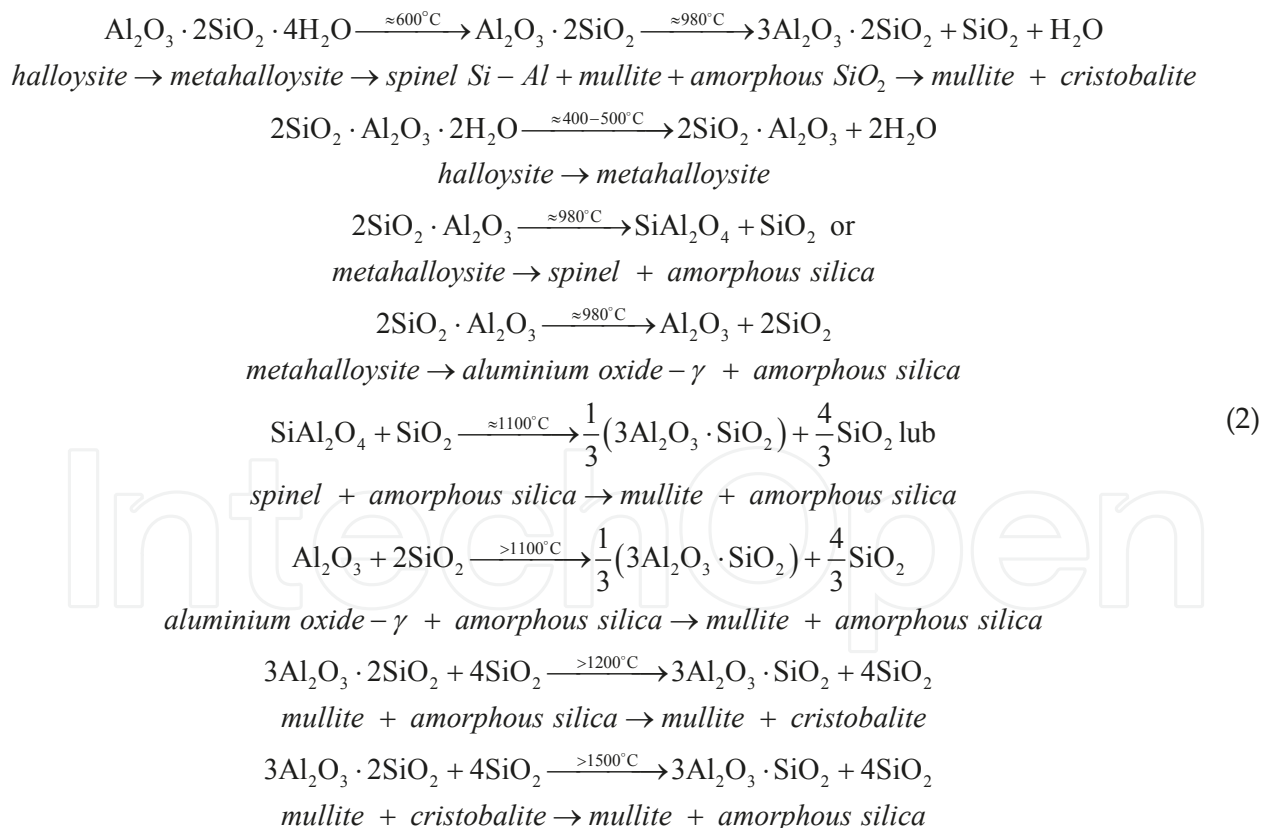
Considerable progress witnessed for years in the development of metallic composite materials, closely linked to the fast growth of the motor industry, is constantly necessitating a search for new, better constructional solutions, which would be lightweight, and also reliable and highly strong, as well as for new composite materials suitable for this purpose. Although pressure-infiltrated composite materials reinforced with different fibres and particles are highly popular, research works have been conducted all the time into selection of new materials for porous skeletons for the reinforcement of metal matrix composite materials. Research into the development of technologies of such materials with sintered porous ones based on halloysite nanotubes, whose potential application possibilities are still being investigated, is inscribing into the former research. Such works are becoming even more important in Poland because this is the place where, apart from the USA and New Zealand, one of the three global deposits of halloysite, that is, nitrided aluminium silicide $\text{Al}_2\text{Si}_2\text{O}_5(\text{OH})_4 \cdot \text{H}_2\text{O}$, that is, a clay mineral of volcanic origin from the group of kaolin fossils, is located. The investigations carried out indicate that nanotubes obtained from halloysite may be an alternative reinforcement of composite materials, for instance with respect to much more costly carbon nanotubes. A reason supporting the use of halloysite nanotubes as a reinforcement of unique aluminium alloy matrix composites is that composite materials can be achieved with a structure at a nanoscale,

having exceptional thermal properties which, unlike composite materials reinforced with, for example, ceramic particles, are characterised by high thermal conductivity whilst maintaining low linear expansion. Thermal stability enables to use this type of material for car engine components such as engine blocks, pistons, cylinders, brake discs, with relatively better heat exchange intensity, by improving heat conductivity and the results improved machine performance. Nanostructured composites reinforced with halloysite nanotubes can, therefore, be competitive to hypereutectic silumins and Al/SiC, Al/Al₂O₃ composites used for this aim.

Halloysite is built of plates with a flat surface, partially rolled or in form of tubes, formed from rolled plates, which is related to mismatch between a tetrahedral layer and a octahedral layer making up the packet [36]. Two types of this mineral are distinguished [36]:

- hydrated halloysite-1 nm, having water in the inter-packet space, featuring low durability dependent on humidity and undergoing transformation into metahalloysite already at room temperature;
- dehydrated halloysite 0.7 nm, called metahalloysite.

If halloysite is heated at temperature above 980°C, structural transformation of halloysite into mullite is seen according to the simplified formula [75]:



Mullite is aluminium silicate 3Al₂O₃·2SiO₂ obtained after sintering minerals containing aluminium oxide and silicon oxide in right proportions, for example, sillimanite, cyanite,

andalusite and also mixtures of kaolin and aluminium oxide. It has been used successfully as an ingredient of refractory and electro-insulating materials and as a ceramic phase reinforcing metallic composite materials, including nanostructured composite materials with an aluminium alloy matrix [12, 76]. A possibility to use mullite for this task was a reason why attempts were undertaken to apply the nanotubes obtained from halloysite, in which transformation will take place—during thermal processes—into mullite. The mullite will be acting as reinforcement in the form of a sintered porous skeleton of aluminium alloy matrix composite materials fabricated by gas-pressure infiltration methods.

Halloysite nanotubes (**Figure 8a**), as an indispensable material in this process, are multiwalled, cylindrical, hollow objects with the diameter less than 100 nm and length of about 500 nm to over 1.2 μm [11, 24]. They are sourced from fossil halloysite and have been widely employed in, for example, ceramic [77, 78], construction, fertiliser and cosmetic branch, for environment protection as universal mineral sorbents, coagula for water treatment, waste stabilisers and in biomedicine as medicine carriers [79, 80]. Halloysite nanotubes have been applied as reinforcing nanocomposites to a small degree only, and mainly for polymer matrix composites in which, when added in several to more than ten per cents, rigidity, fireproofness, strength, hardness, thermal stability, and in some cases also electrical conductivity, are improved [80, 81].

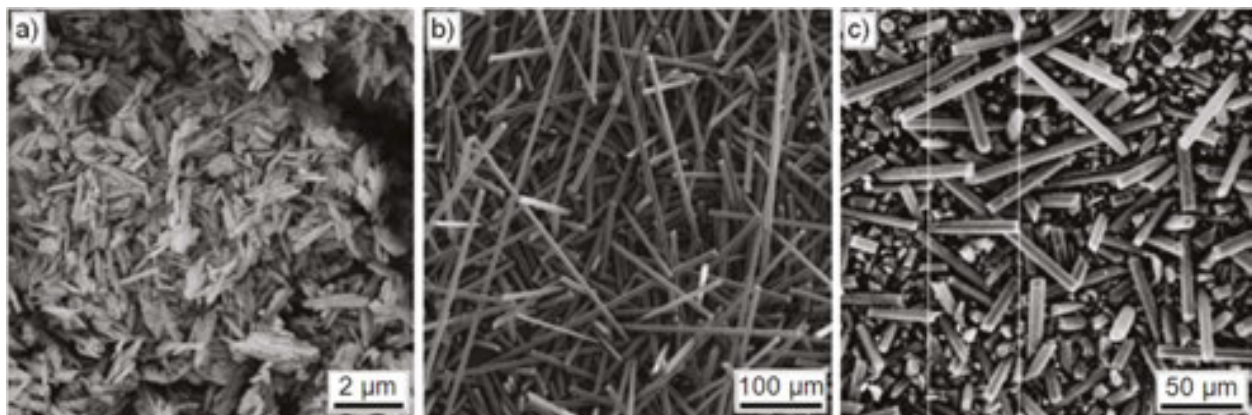


Figure 8. Morphology of base powders of: (a) halloysite nanotubes, (b) carbon fibres, (c) mixture of halloysite nanotubes made of carbon fibres with mass fraction of 50% after 5 min of mechanical milling in ball mill.

It was found as a result of own investigations that—through the pressure infiltration with a liquid aluminium alloy of porous ceramic skeletons fabricated by sintering halloysite nanotubes together with an agent forming the open structure of pores; by selecting appropriately the conditions of powder preparation, compression, sintering and pressure infiltration and a fraction of halloysite nanotubes, as a result of structural transformations taking place in sintering and pressure infiltration—it is feasible to achieve aluminium alloy matrix composite materials, reinforced with a sintered mullite porous skeleton, with enhanced mechanical properties and wear resistance, much higher than the functional properties of the matrix material. An outcome of such own works is that properties were identified and the structure was developed and created of a new generation of composite materials infiltrated by the gas-pressure method, reinforced with porous skeletons produced using the mechanical synthesis,

consolidation and sintering of a mixture of powders consisting of halloysite nanotubes and carbon fibres as a foaming agent, and also influence was identified by the reinforcing phase fraction on the structure and mechanical and functional properties of the so-developed engineering materials.

Porous ceramic skeletons, being the final reinforcement of composite materials with an EN AC- AlSi12 alloy matrix, were fabricated by the mechanical milling, compression and sintering of halloysite nanotubes supplied by NaturalNano (USA). Powders were prepared in order to fabricate porous ceramic skeletons, by the mechanical dry milling of a mixture of halloysite powder with an agent forming the structure and size of open and interlinked pores. Sigrafil CIO M250 UNS carbon fibres by SGL Carbon Group (Germany) were used for this purpose. The morphology of the carbon fibres used is presented in **Figure 8b**. Five sets of materials were prepared containing, respectively, a 30, 40, 50, 60 and 70% volume fraction of halloysite nanotubes (**Figure 9**). A slipping agent in the form of powdered micronised amide wax, MA7050, with a volume fraction of 1% was additionally used to change the rheological properties of the powder mixture. The task of the slipping agent is to decrease adhesion between the powder material, and a mill and grinding mediums, and also to eliminate friction between the die walls and powder particles, which is impeding pressing and production of cohesive mouldings. A centrifugal ball mill, Pulverisette 5, by Fritsch company, was used to produce a crushed and homogenous powder mixture. Milling time was selected by analysing the bulk density of the prepared powder mixtures and their morphology (**Figure 9**). As bulk density, related to milling time, was decreasing, a mixture of powders after 15 min of milling was selected for further investigations. The prepared powder mixtures were formed by cold uniaxial pressing in closed (circular and rectangular) dies on a platen hydraulic press, LabEcon 600 Fontijne Grotnes. The diameter of a die socket with round section was 30 mm, and the dimension of the rectangular die socket was 12×35 mm. The specimens were pressed under the pressure of 25–150 MPa with steps for every 25 MPa. The pressing time was 15 s. The influence of the applied pressing pressure was judged by the appearance of mouldings (no cracks, losses, delamination, etc.), and their strength allows to lay them on a ceramic base for subsequent sintering in a heating device. Low pressing pressure of only 25 MPa does not ensure suitable powder compression, which will have influence on cracking and chipping of the specimens' edges when removing them from the die. On the other hand, the mouldings pressed under a high pressure of 125 and 150 MPa were distinct for delamination, which was particularly visible near the front surface of the moulding, to which a working stamp was acting. It was therefore decided that the pressing pressure of 50–100 MPa will be applied. The materials pressed in such conditions are free of defects and possess suitable strength, and also porosity after sintering, as it is essential to maintain high density of open pores in the whole volume of the sinter for its infiltration. The pressing pressure was further selected by examining the shape of the pressed and sintered mouldings due to high distortion resulting from inhomogeneous shrinkage in sintering. It was initially assumed that a low pressing pressure will ensure the necessary strength of mouldings and the high porosity of the sintered specimens. Particles are more compressed due to a higher pressure applied, as a result of which the effect of shrinkage is smaller. Sinter infiltration takes place despite smaller pores; hence, it seems that such a solution is less favourable.

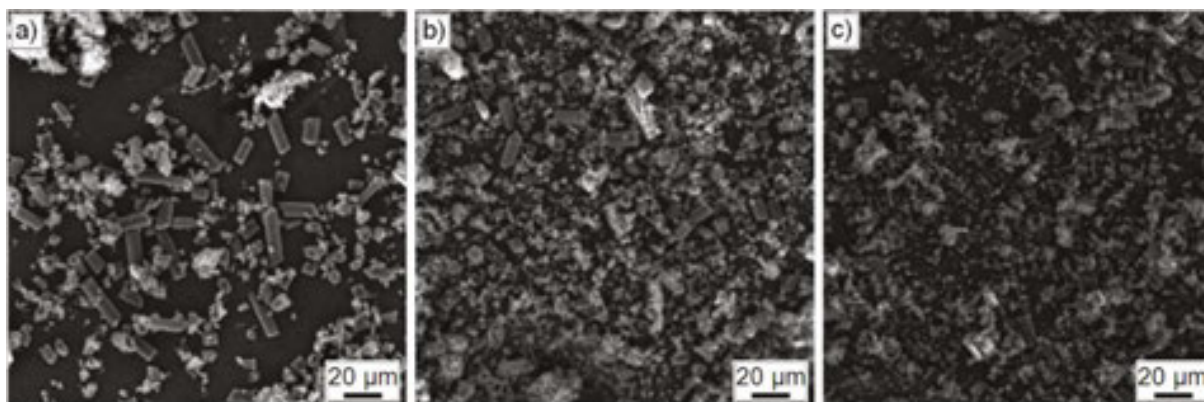


Figure 9. Morphology of mixture of halloysite nanotubes with 50% volume fraction of carbon fibres, after: (a) 30, (b) 120 and (c) 300 min of mechanical milling in ball mill.

The porous ceramic skeletons for pressure infiltration were sintered in a high-temperature oven, PRS 75W, in the atmosphere of air with a flow rate of 5 l/h, as a result of slow heating to the carbon fibre degradation temperature, heating at 800°C, selected based on a thermogravimetric curve analysis (**Figure 10a**), to degrade carbon fibres within the whole volume of the specimens, reheating to the appropriate sintering temperature, sintering and then cooling. Sintering temperature was chosen based on the results of examinations in a high-temperature microscope and derivatograph. By assuming that the melting point of the mullite formed from the applied halloysite is about 1830°C, this material should be sintered within the range of 915–1465°C, and as ion bonds and/or covalent bonds exist, it may reach even 1620°C. As mullite is not characterised by pure covalent bonds, it was thus assumed that the maximum sintering temperature will be 1500°C. Theoretically, the investigated material should be sintered at relatively low temperature at which the diffusion of atoms occurs on the surface of particles, which is the main transport mechanism of the matter. The surface of the necks connecting ceramic particles is then expanding, but the whole particles are not brought closer, and thus, an undesired effect of shrinkage does not take place (**Figure 10b**). A small rate of diffusion requires long heating times (of several dozen of hours), which is economically ungrounded. If a higher temperature of sintering is applied, diffusion certainly occurs in the examined sintered material along the grain boundaries, and volumetric diffusion occurs, which is responsible for sinter shrinkage caused by the particle centres coming closer. Halloysite nanotubes were pressed under the pressure of 100 MPa for 15 s and then heated in an oven at 100, 300, 500, 800, 1100, 1300 and 1500°C for 1 h. Shrinkage in the range of 100–1500°C could be calculated as moulding diameter dimensions changed, and the shrinkage was 22.2%. 0.07 g of halloysite nanotubes were subjected to thermogravimetric tests in the range of 20–1500°C in the atmosphere of air. It was discovered when analysing a thermogravimetric curve and its derivative that an endothermic reaction takes place while heating the halloysite nanotubes within the temperature range of 400–600°C (maximum at 516°C), and the reaction is associated with dehydroxylation and decomposition of halloysite to metahalloysite (loss mass of approx. 17%), and an endothermic reaction takes place at approx. 980°C, associated with the halloysite structure reconstruction and the creation of a spinel Si-Al phase as a transient form [36, 57, 82]. Linear changes in the function of temperature were examined with a high-temperature microscope by Leitz by the

microscope-photographic method within the temperature range of up to 1600°C in the atmosphere of air with a heating rate of 5 and 8°C/min. In order to establish sintering temperature, pristine halloysite nanotubes and their mixtures with carbon fibres were formed manually under the pressure of 3 and 100 MPa. A series of photos presenting the behaviour of the material during heating was obtained while continuously observing and recording photographically changes in its shape and dimensions (shrinkage, expansion or local swelling) in the function of temperature, as an approximate simulation of the phenomena taking place in the examined material when producing porous ceramic skeletons. The recorded material changes were analysed with image conversion and analysis algorithms. Mouldings of mineral halloysite nanotubes pressed manually without additives (a binder in the form of water present in the structure) were examined in a high-temperature microscope in an oxidising atmosphere. The mouldings were heated at a rate of 8 and 5°C/min at 20–1600°C with recording every 100°C (**Figure 10c**). The slower heating of the material containing water in its structure does not cause abrupt volumetric changes of the moulding, and it supports its intensive shrinkage, though.

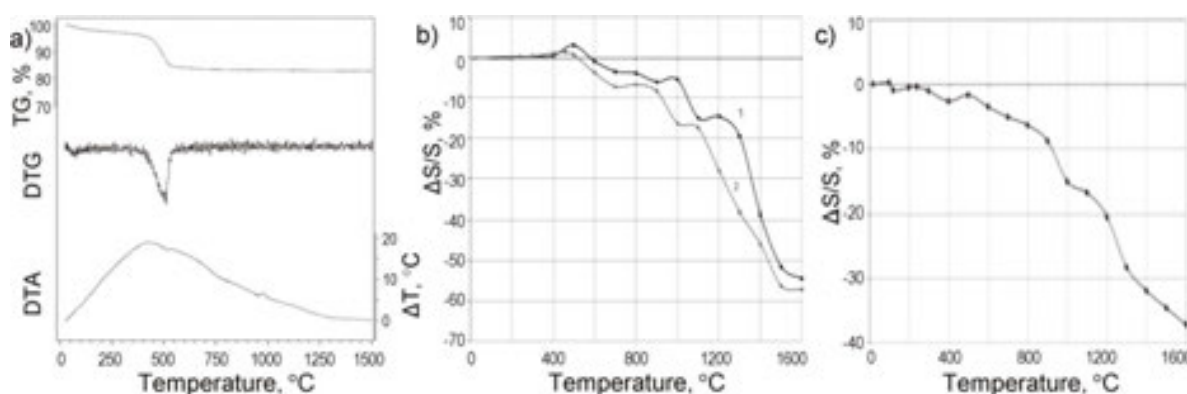


Figure 10. (a) Thermogravimetric curve (TG), differential thermogravimetry curve DTG and differential thermal analysis curve (DTA) of halloysite nanotubes (TG = 100 mg, $m_0 = 70$ mg, 7.5°C/min, rel. 96), (b) comparison of changes in the dimensions of moulding of halloysite nanotubes $\Delta S/S$, pressed under the pressure of 3 MPa without additives; heating rate of 1–8°C/min and 2–5°C/min, (c) changes in the dimensions $\Delta S/S$ of moulding containing halloysite nanotubes (70%) and carbon fibres (30%) pressed under the pressure of 100 MPa with Microwax slipping agent added; heating rate of 5°C/min.

No occurrence of characteristic temperature (softening, melting nor flow) of halloysite nanotubes was found for mineral halloysite due to their high melting point of approx. 1800°C. A change in the dimensions of mouldings for the temperature range of 1000–1600°C (**Figure 10b, c**) was found, however, due to large impact of the water contained in the structure of halloysite nanotubes. The material shows nearly linear thermal expansion to the temperature of 500°C. The first phase of shrinkage occurs above that temperature associated with halloysite dehydroxylation and the formation of the metahalloysite phase [82]. Another shrinkage occurs at 900°C, and dimensional stabilisation occurs within the range of 1000–1100°C, referred to as stability plateau, connected with crystallisation of the intermediate phase—spinel Si-Al. When halloysite is further heated, this causes the transformation of spinel $2Al_2O_3 \cdot 3SiO_2$ into mullite $3Al_2O_3 \cdot 2SiO_2$ with formless glazed silica SiO_2 formed at the same time, which activates sintering (**Figure 11**). A structure comprised of mullite crystals deposited in the amorphous

silica or cristobalite is produced above 1100°C (Figures 12, 13). The mouldings of mixtures of halloysite nanotubes with a 50 and 30% (Figure 10c) fraction of carbon fibres pressed under the pressure of 100 MPa, that is, in conditions simulating the sintering of mouldings, were also examined in a high-temperature microscope in an oxidising atmosphere.

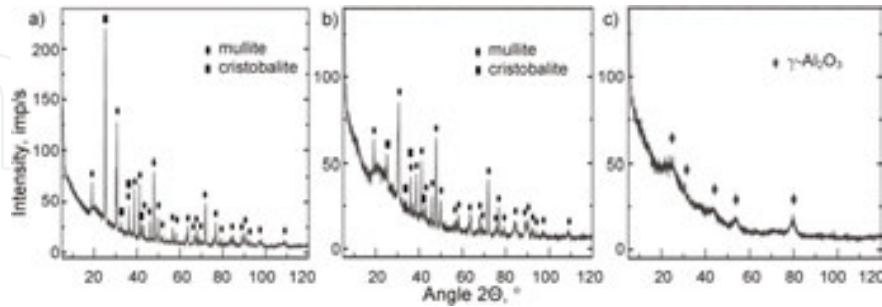


Figure 11. The results of X-ray phase analysis of porous ceramic skeletons with volume fraction of 70% of HNT, pressed under the pressure of 100 MPa and sintered in temperature of (a) 1500°C, (b) 1300°C, (c) 1100°C.

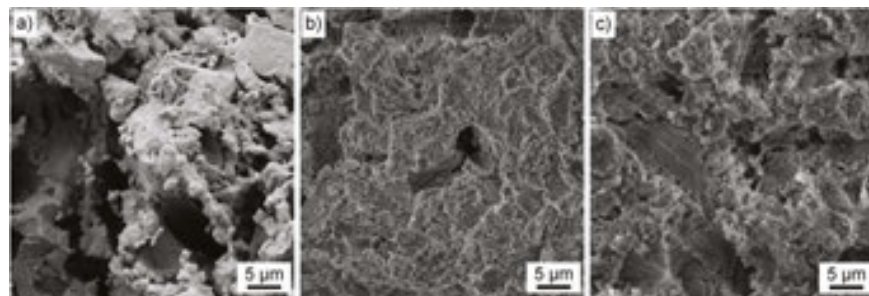


Figure 12. The morphology of porous ceramic skeletons with volume fraction of 70% of HNT, pressed under the pressure of 100 MPa and sintered in temperature of (a) 1500°C, (b) 1300°C, (c) 1100°C.

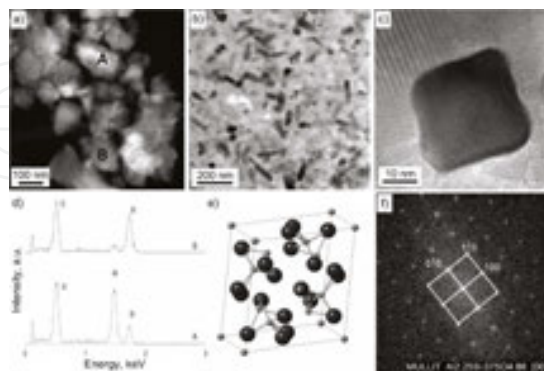


Figure 13. The structure of porous skeletons sintered at the temperature of 1500°C—mullite grains: (a) HAADF image, (b) TEM-BF image of porous skeleton, (c) high-resolution image STEM-HAADF of mullite grain in orientation [001], (d) comparison of chemical composition analysis results in two areas shown in Figure a (B—atomic percentage of atoms: Al—28%, Si—13%, O—69%), (e) model of elementary cell of $\text{Al}_{2.25}\text{Si}_{0.75}\text{O}_{4.87}$ phase, (f) FFT piece of image shown in Figure c.

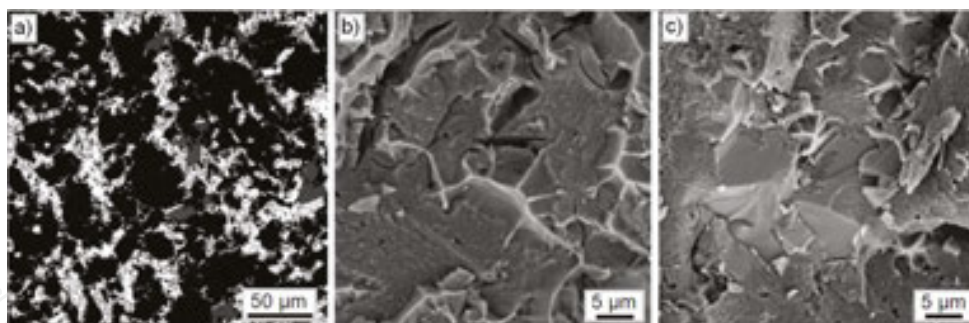


Figure 14. (a) Structure of composite materials reinforced with porous ceramic skeletons with the mass fraction of 70% HNT, pressed under the pressure of 100 MPa and sintered at the temperature of 1500°C; (b, c) structure of fractures of composite materials as in **Figure a**, with mass fraction of HNT of: (b) 50%, (c) 70%.

The presence of a solid solution of aluminium α -Al and silicon eutectics $\alpha+\beta$, being a matrix of composite materials and a ceramic phase—mullite $3\text{Al}_2\text{O}_3 \cdot 2\text{SiO}_2$, whose reflexes come from reinforcement in form of sintered skeletons, was found as a result of an X-ray structural analysis in the composite materials reinforced with skeletons made by the sintering of halloysite nanotubes. The structure of such composite materials is characterised by uniform distribution in the reinforcement matrix produced by sintering the halloysite nanotubes, and by the nearly full filling of pores with a liquid aluminium alloy (**Figure 14**), whereas manufacturing conditions of porous reinforcing skeletons do not exert significant impact on the structure. Significant structural differences are caused by variations in the sintering temperature of such skeletons. Numerous precipitates of coarse-grained silicon occur as a result of sintering at 1300 and 1500°C, having a tendency to crystallise on the surface of the ceramic phase, whose share increases as the fraction of reinforcement increases. The crystals of mullite $3\text{Al}_2\text{O}_3 \cdot 2\text{SiO}_2$ (**Figure 13**) are present inside the composite material grains, along with irregularly shaped pores and those having the diameter of approx. 100 nm, whose morphology may indicate empty areas after cristobalite grains SiO_2 , which were subjected to decomposition in the infiltration process. This may be evidenced by the presence of occasional precipitates with a heightened concentration of silicon and oxygen, which indicates the presence of cristobalite SiO_2 . The presence of 3 main components of the composite material obtained, that is, silicon, aluminium solution and mullite $3\text{Al}_2\text{O}_3 \cdot 2\text{SiO}_2$, was also confirmed with the EDS method in a scanning microscope (**Figure 15**). About 200 nm thick transition zone exists between aluminium solid and mullite $3\text{Al}_2\text{O}_3 \cdot 2\text{SiO}_2$ with relatively large grains, larger than mullite grains in the external—from the side of mullite—part of the transition zone, with the presence of an aluminium solution and oxygen and a lower concentration of silicon in relation to mullite (**Figures 15, 16**). As the SiO_2 phase is thermodynamically unstable in the presence of aluminium, it is reacting with it by creating aluminium oxide [83]. Coarse-grained precipitates of pure silicon are created as a result of aluminium acting with cristobalite SiO_2 during infiltration and diffusion, and the structure of an aluminium solution of the matrix corresponds to the structure of a hypereutectic alloy. The newly created precipitates of silicon are crystallising from an Al-Si alloy on the matrix-reinforcement boundary, and due to their higher strength in relation to matrix strength, their nucleation contributes to the reinforcement of the separation boundary. Following the infiltration and decomposition of cristobalite SiO_2 ,

mullite $3\text{Al}_2\text{O}_3 \cdot 2\text{SiO}_2$ constitutes basically the only component of a ceramic skeleton which is not subject to changes. The expected interaction between liquid aluminium and mullite $3\text{Al}_2\text{O}_3 \cdot 2\text{SiO}_2$ does not take place, therefore. This may result from infiltration conditions, that is, the flushing temperature of a liquid alloy, which is not higher than 800°C , and from a rate of infiltration and evacuation of heat directly after it, otherwise as it takes place during wettability tests or pressureless infiltration.

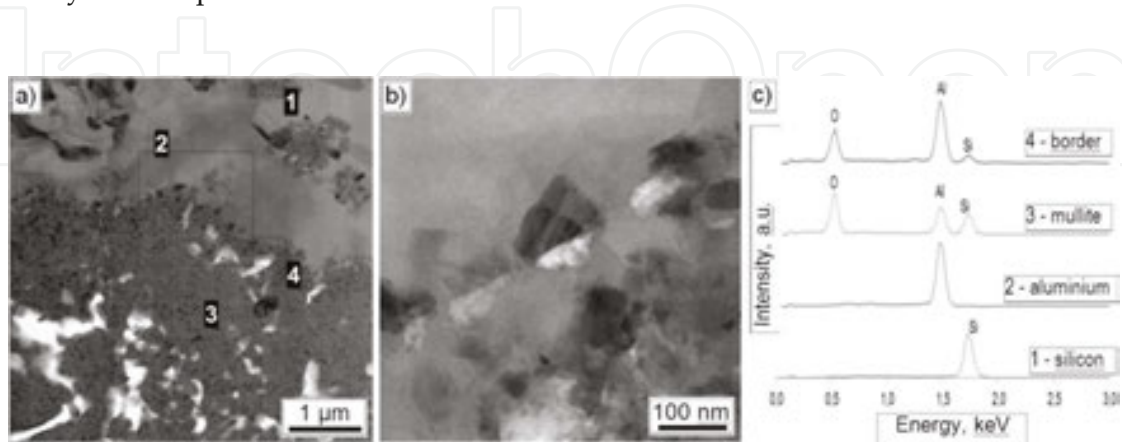


Figure 15. (a, b) Image of structure of composite material reinforced with porous skeletons, magnified pieces with transition zone between ceramics and metal, (c) results of chemical composition analysis in four areas marked in **Figure a**.

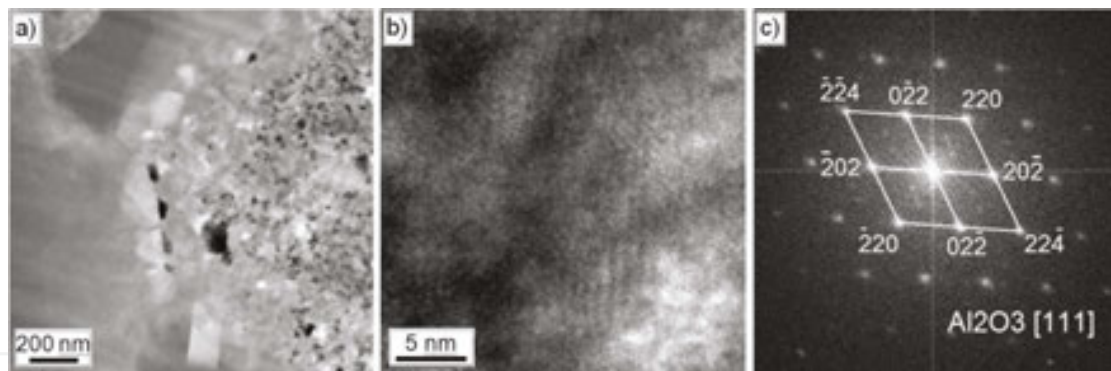


Figure 16. Transition zone between metal and ceramics: (a) STEM-BF image of area of transition zone, (b) HRTEM image, (c) Fourier transform with diffraction image solution.

As the fraction of reinforcement is increasing in the form of a porous skeleton of mullite $3\text{Al}_2\text{O}_3 \cdot 2\text{SiO}_2$ obtained as a result of sintering the halloysite nanotubes, the hardness of the composite materials produced as a result of pressure infiltration is rising. The highest hardness of 114.6 HRF is seen for materials obtained by infiltrating sintered skeletons at 1500°C with a 70% fraction of ceramic phase, whilst the lowest, of 64.9 HRF, for materials reinforced with skeletons sintered at 1100°C . A twice higher value of hardness results from the difference in the structure of ceramic skeletons, depending on their sintering temperature. The bending strength of the analysed composite materials is increased considerably as compared to the strength of an EN AC- AlSi12 alloy forming the matrix, which is 224–276 MPa in case of reinforcing with skeletons sintered at the temperature of 1300°C with a 60% fraction of HNT,

and to 307 MPa after sintering porous skeletons at 1500°C with a 50% fraction of HNT. When the fraction of reinforcement is increased, the bending strength of the discussed composite materials is decreased.

6. The structure and properties of sintered titanium porous skeletons obtained by selective laser sintering and aluminium alloy matrix composite materials reinforced with them

This sub-chapter presents the possibility of manufacturing sintered porous skeletons by an additive manufacturing technology (Figure 17). Procedural benchmarking techniques with a dendrological matrix of technology value were used for selection of a porous material manufacturing technology [84–86]. The potential of additive technologies is much higher than of other technologies, and it is represented by opportunities ensured by 3-D design, which allows to almost fully control the materials produced in respect of their structure, dimensions and the shape of pores, and the repeatability of geometrical characteristics. The additive manufacturing technology produces no wastes and is comprised of two main stages of design and manufacture, which is also greatly improving the potential of such technologies in the aspect of porous material fabrication.

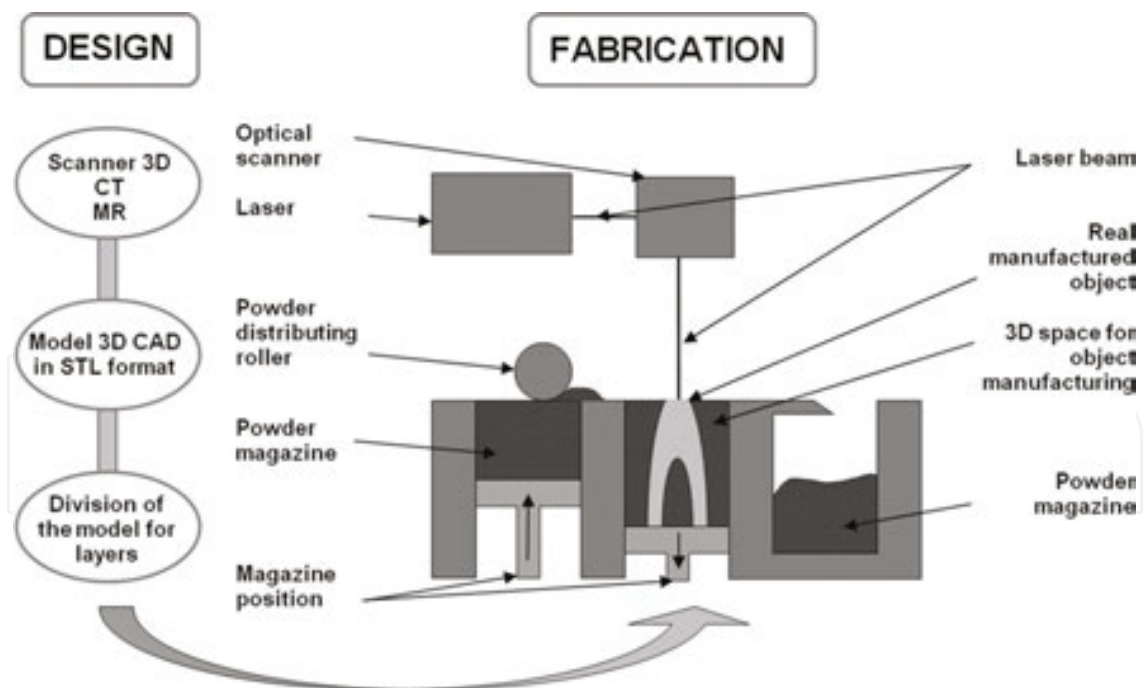


Figure 17. Selective laser sintering technology process diagram.

The attractiveness of the particular additive manufacturing technologies does not differ much. A comparative analysis result indicates SLS—selective laser sintering, and SLM—selective laser melting technologies, as having the best set of characteristics for the fabrication of metallic

porous materials. The attractiveness and potential coordinates are ranking these technologies in the wide-stretching oak quarter with the highest potential and attractiveness, thus with the best development outlooks. All the results presented below relate to pristine titanium. Titanium was chosen for its attractive properties, including anticorrosive resistance, biocompatibility, good relationship between strength and mass and due to its broad range of applications in various industries starting with the space, aviation and car industry through medicine to dentistry. For this reason, porous titanium skeletons with an adequate group of properties can find their application in different industries. The real motivations for those investigations were originally connected with the creation of biological and engineering composite materials and implant-scaffold materials planned for application in regenerative medicine and dental implantology [65–70, 74, 87–90]. The results of such investigations were next extended to develop a new group of composite materials with a metal alloy matrix, mainly aluminium, reinforced with porous skeletons made of titanium and its alloys, for example, Ti6Al4V and Ti6Al7Nb sintered by SLS/SLM, although powders of other metals such as stainless steel, cobalt and chromium alloys and others can also be used to produce reinforcement. The AM 125 system by RENISHAW with AutoFAB software was used for manufacturing porous skeletons by SLS/SLM. The YFL fibre laser with an active material doped with Ytterbium and the maximum power of 200 W was used in the AM 125 device. The AM 125 system is equipped with a vacuum chamber enabling to apply a unique device working chamber emptying method in such a manner that first all gases are pumped off from the working chamber, and then inert gas, for example, argon or nitride, is introduced. A working environment is created with such a sequence of operations, almost free of any oxygen, where such reactive materials as titanium and titanium alloys can be sintered. The level of the consumed inert gas is minimised by using a fully tight, welded working chamber. The AM 125 instrument features a powder container with automatic valves supplying additional portions of powder during the whole process, while the excess powder—when another layer is distributed in the working chamber—is diverted to a special container that is quickly and easily detachable and can be placed in a powder sieving or selecting station, and hence, the powder can be re-used in the next process. The time needed to produce the designed model depends on its size, structural complexity, as well as the number of elements which are made in a single process. The fabrication accuracy of models depends on the laser power applied: for the layer thickness of 20–50 μm , it is $\pm 20 \mu\text{m}$ in the XY plane for low laser power and $\pm 100 \mu\text{m}$ for high laser power.

The AM 125 instrument is also integrated with suitable software for Manufacturing Applications 3D Marcarm Engineering Autofab for computer-aided design/manufacturing CAD/CAM for rapid manufacturing technology with the SLS technique enabling to adapt the model designed to the fabrication conditions and to achieve the characterised properties. A 3-D model recorded in the stereolithography STL format permitting to produce items by a layered technique should be the outcome of such designing. Once the model reaches the appropriate size and structure, the whole model is divided into layers with specific thickness. The number of layers reflects the number of powder layers, which are sintered until a ready element is achieved. AutoFab software enables to determine optimum manufacturing conditions, among others, layer thickness, laser power, laser beam diameter, scanning rate, distance between par-

ticular remelting paths. More and more complicated shapes with a specific internal and external structure can be manufactured with the software available, which allows designing in three-dimensional space. Once all manufacturing conditions/characteristics are set, the model designed is transferred into the machine's software, where selective laser sintering is performed. The software allows for nearly complete control of the size, geometrical features, and also repeatability of the designed items and to fully control manufacturing conditions by steering them within their relevant applicability range.

The SLS technology is essentially an advanced powder metallurgy technology where the element constitution process begins with spreading a powder layer across the table with its position adjustable in relation to the axis z . The layer acts as a substrate for the item being created. A laser beam is guided across the powder surface according to the pre-entered and adequately configured information concerning the particular layers of the cross-spatial section of the part image. Next, the table with the powder is lowered by the user-defined height corresponding to the layer thickness, and another thin layer of powder is spread, where grains are again sintered/melted by remelting the particles of the new powder on the surface with the existing piece of the item being constituted. The successive layers of the cross section are intersintering/intermelting. The cycle is repeated until finishing to constitute a complex element, after which temperature is lowered, and the element produced is removed from the powder bed and subjected to finishing depending on its use, for example, sanding or polishing. Such an element has a nonuniform inner structure which allows to work it further and join with other materials, for example, a ceramic or metallic material, by infiltration.

Titanium powder Grade 2 with the grain size of up to $45\ \mu\text{m}$ with spherical shape was used for selective laser sintering to produce porous skeletons (**Figure 18a**). The powder applied has a reduced concentration of oxygen to 0.14%. The concentration of oxygen in the working chamber during sintering is lowered, as appropriate, below 100 ppm.

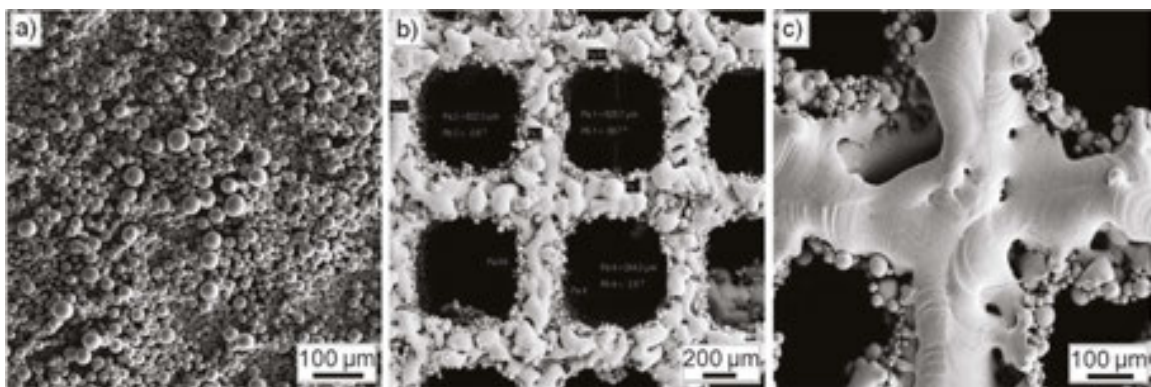


Figure 18. (a) Titanium powder with grain size of $0\text{--}45\ \mu\text{m}$; surface typography of porous titanium skeletons with different pore size: (b) $630\ \mu\text{m}$, (c) $350\ \mu\text{m}$; SEM.

A pool of base unit cells was used for designing porous titanium skeletons (**Figure 19**) which – by copying and selecting appropriate lattice values such as height, depth and width, allowed to define the structure of porous skeletons with the pore size of $250\text{--}750\ \mu\text{m}$. A hexagon cross

unit cell (**Figure 19a**), whose main advantage is a special reinforcement in a node connecting the individual skeleton fibres, was selected for producing porous titanium elements in SLS technology.

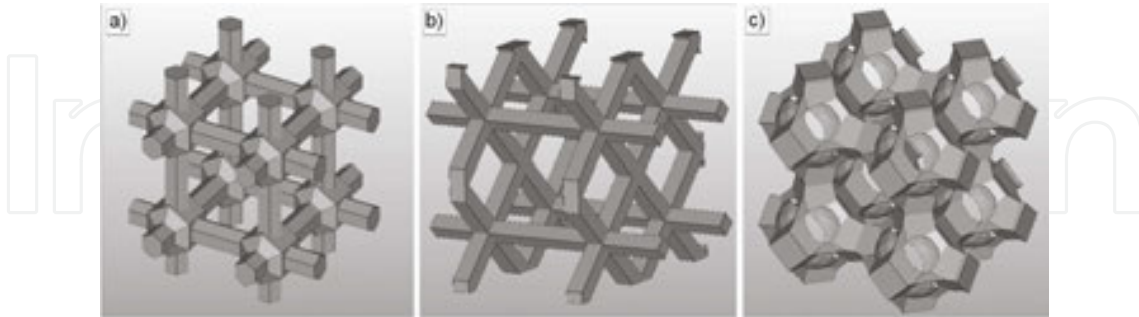


Figure 19. Examples of base unit cells with different spatial structure: (a) hexagon cross, (b) diagonal cross, (c) spherical.

Titanium skeletons were fabricated with the average pore size of ~ 250 , ~ 350 i ~ 450 μm and a unit cell dimension of, respectively, 500, 600 and 700 μm , with a different arrangement of unit cells in the space relative to the axis of the system of coordinates (**Figure 20**) at the angle of 0° to the start of the system of coordinates, 45° relative to the axis x of the system of coordinates, 45° to the axis y, 45° to the axis x and 45° to the axis y, 45° to the axis y and 45° to the axis x.

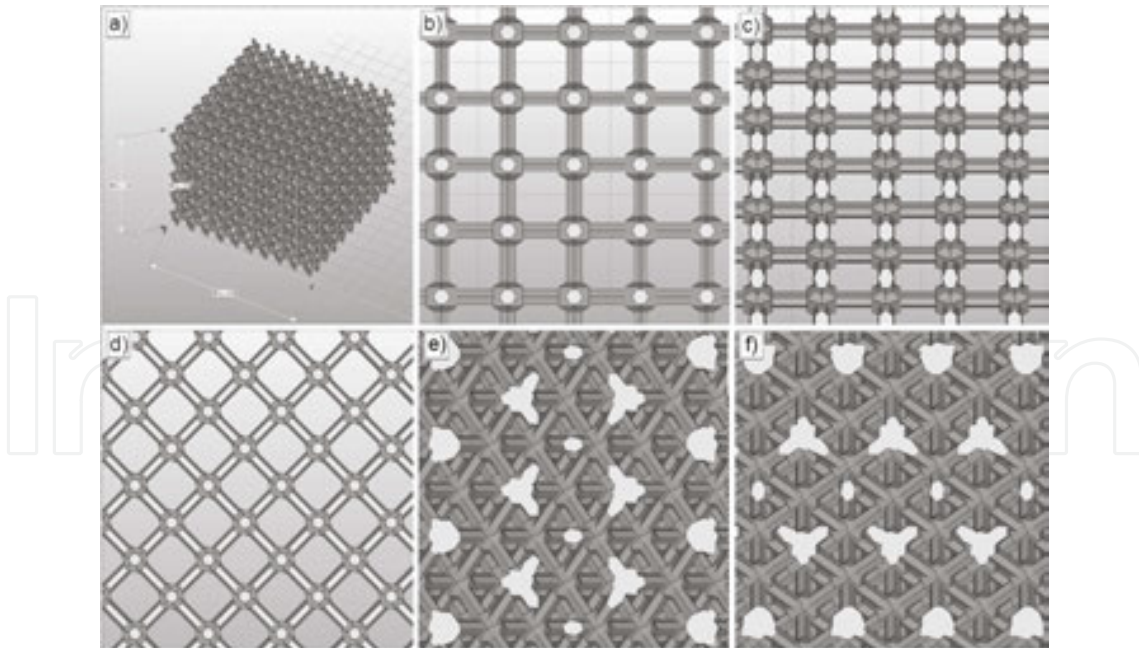


Figure 20. (a) Models of porous elements sized $10 \times 10 \times 5$ mm; image of structure of computer models presenting the arrangement of base unit cells in the space of the system of coordinates: (b) at the angle of 0° to the start of the system of coordinates (symbol A), (c) at the angle of 45° relative to the axis x (symbol B), (d) at the angle of 45° relative to the axis y (symbol C), (e) at the angle of 45° relative to the axis x and 45° relative to the axis y (symbol D), (f) at the angle of 45° relative to the axis y and 45° relative to the axis x (symbol E).

The surface topography of porous titanium skeletons depends on the size of pores (**Figure 18b, c**), on the arrangement of unit cells relative to the system of coordinates (**Figure 21**), and also on chemical etching in an aqua regia solution (volume ratio of HCl:HNO₃ of 3:1) or in a 14% water hydrofluoric acid solution, in order to avoid partial melting on the surface and fine powder particles not bonded permanently with the previously constituted element (**Figure 22**). The roughness of porous skeletons before etching is much higher than after etching. The strength properties of the porous skeletons sintered by SLS from titanium powder depend on the size of pores and their spatial orientation (**Figure 23**).

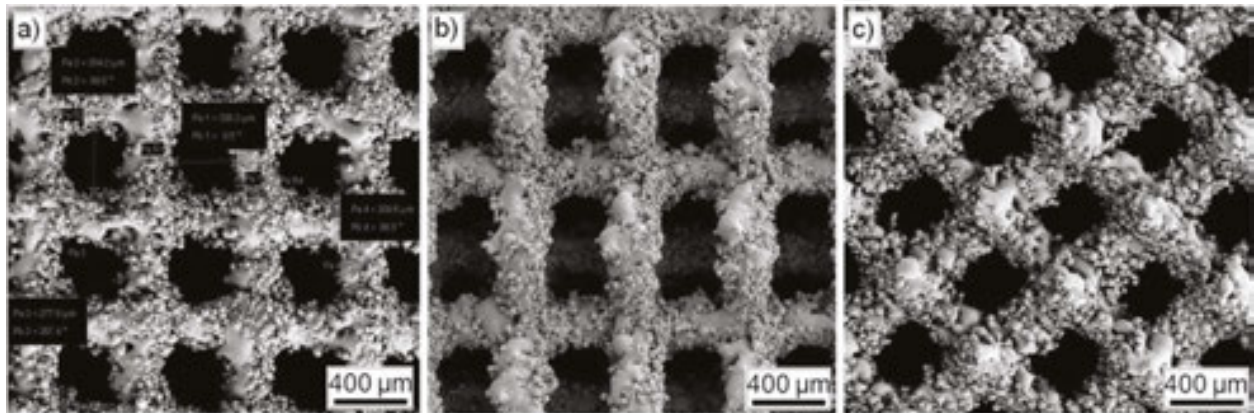


Figure 21. The surface topography of porous titanium skeletons with the pore size of 350 μm and different orientation of unit cells in relation to the system of coordinates: a) at the angle of 0° to the start of the system of coordinates, b) at the angle of 45° relative to the axis x, c) at the angle of 45° relative to the axis y; SEM.

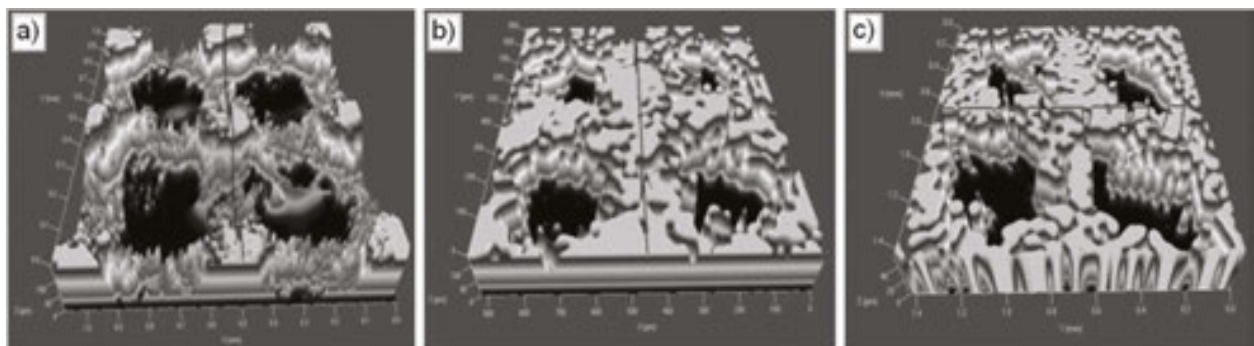


Figure 22. The surface topography of porous titanium skeletons with the pore size of: (a, b) 250 μm, (c) 450 μm; (a) without etching, (b, c) after etching in aqua regia; confocal microscope.

A lightweight titanium skeleton with the porosity of approx. 60%, distinct geometry and compressive strength of approx. 125 MPa, was produced using appropriate fabrication conditions (laser power, laser beam diameter, exposure time of powder to laser activity). Porous titanium skeletons were used for fabrication of composites by infiltration at tempera-

ture of 800°C with an EN AC- AlSi12 alloy and, respectively, EN AC- AlSi7Mg0.3 alloy, under the pressure of 2–3 MPa for 2 min; hence, composites with a new set of properties were obtained.

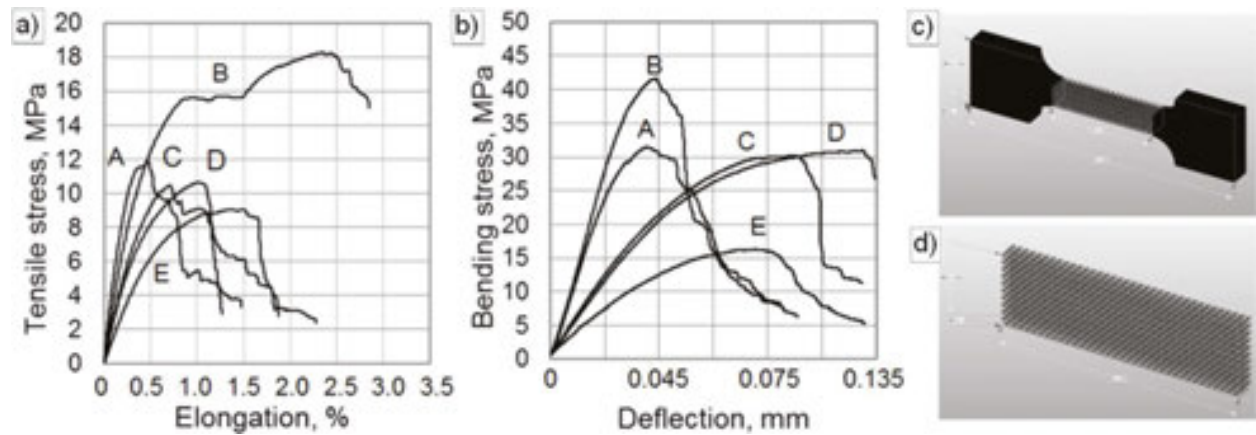


Figure 23. Progression dependency of strength curves: (a) tensile strength, (b) bending strength of skeletons with the pore size of 350 μm sintered by SLS method from titanium powder (marked as in **Figure 20**), (c, d) specimens with porous measuring part: (c) for stretching, (d) for bending.

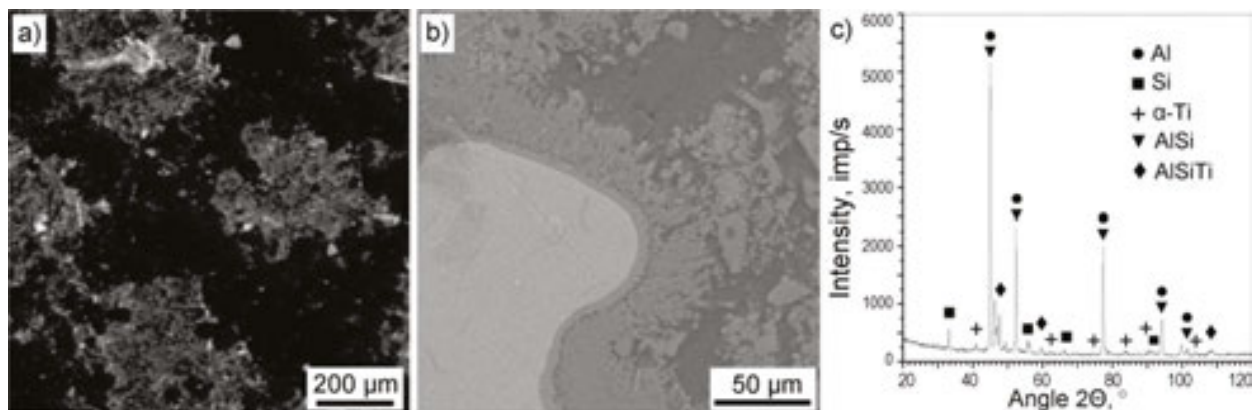


Figure 24. Structure of AlSi12/Ti composite material; (a) stereoscope microscope, (b) SEM, (c) X-ray diffraction pattern.

The structure of the sintered EN AC- AlSi12 and EN AC- AlSi7Mg0.3 aluminium alloy matrix composite material (**Figures 24, 25**) reinforced with porous titanium skeletons manufactured by SLS methods confirms that the titanium skeleton pores are thoroughly filled as a result of infiltration. The results for X-ray structural examinations for an AlSi12/Ti composite material (**Figure 24c**) reveal that phases are created between particular composite material components during infiltration. An AlSiTi phase occurs in the composite material as a result, apart from such phases as Al, Si, Ti and AlSi . The so-achieved composite materials exhibit much higher strength properties than a matrix material and the porous skeleton itself (**Figure 25c**). This creates extensive application opportunities for such composite materials.

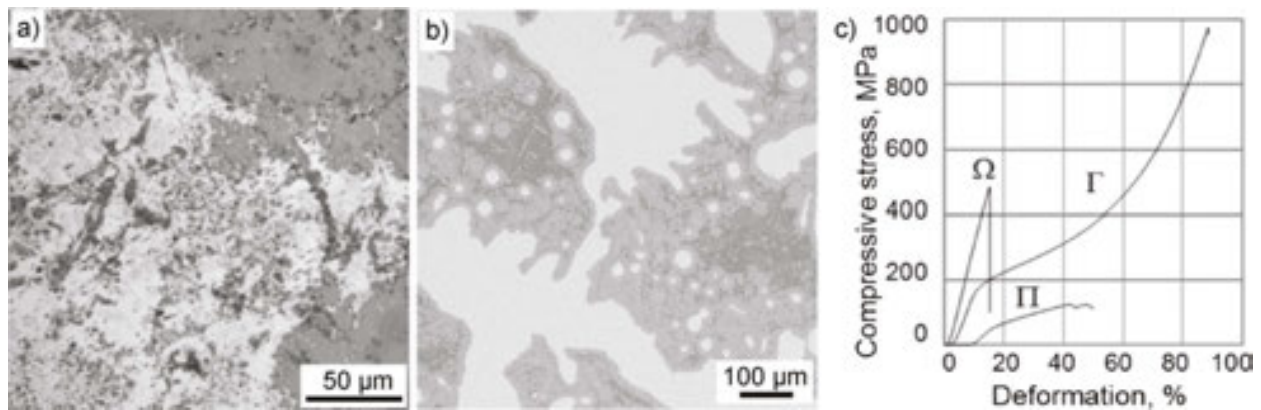


Figure 25. Structure of composite material produced by infiltration of titanium skeleton with AlSi7Mg0.3 alloy; (a) light microscope; (b) SEM; (c) compressive strength, Γ —matrix material, Π —sintered porous material, Ω —composite material.

Author details

Leszek A. Dobrzański^{1*}, Grzegorz Matula¹, Anna D. Dobrzańska-Danikiewicz², Piotr Malara¹, Marek Kremzer¹, Błażej Tomiczek¹, Magdalena Kujawa¹, Eugeniusz Hajduczek¹, Anna Ahtelik-Franczak¹, Lech B. Dobrzański³ and Jagoda Krzysteczko¹

*Address all correspondence to: leszek.adam@gmail.com

1 Silesian University of Technology, Institute of Engineering Materials and Biomaterials, Gliwice, Poland

2 Silesian University of Technology, Institute of Engineering Processes Automation and Integrated Manufacturing Systems, Gliwice, Poland

3 Centre of Medicine and Stomatology 'SOBIESKI', Gliwice, Poland

References

- [1] Kaw AK. Mechanics of composite materials. 2nd ed. Boca Raton: CRC Press, Taylor & Francis Group; 2006. 457 p.
- [2] Dobrzański LA. Engineering materials and materials design. Fundamentals of materials science and physical metallurgy. 2nd ed. Warsaw: WNT; 2006. 1600 p. (in Polish) ISBN 83-204-3249-9
- [3] Chawla KK. Ceramic matrix composites, 2nd ed. Boston: Kluwer Academic Publishers; 2003. 449 p.

- [4] Gibson RF. Principles of composite material mechanics. 3rd ed. Boca Raton: CRC Press, Taylor & Francis Group; 2011. 683 p.
- [5] Kumar HGP, Xavier MA. Graphene reinforced metal matrix composite (GRMMC): a review. *Procedia Engineering*. 2014;97:1033–1040. doi:10.1016/j.proeng.2014.12.381
- [6] Alonso A, Pamies A, Narciso J, Garcia-Cordovilla C, Louis E. Evaluation of the wettability of liquid aluminum with ceramic particulates (SiC, TiC, Al₂O₃) by means pressure infiltration. *Metallurgical Transactions: A*. 1993;24:1423–1432. doi:10.1007/BF02668210
- [7] Książek M, Sobczak N, Mikułowski B, Radziwiłł W, Surowiak I. Wetting and bonding strength in Al/Al₂O₃ system. *Materials Science and Engineering: A*. 2002;324:162–167. doi:10.1016/S0921-5093(01)01305-3
- [8] Mortensen A. Interfacial phenomena in the solidification processing of metal matrix composites. *Materials Science and Engineering: A*. 1991;135:1–11. doi:10.1016/0921-5093(91)90527-T
- [9] Rajan TPD, Pillai RM, Pai BC. Reinforcement coatings and interfaces in aluminium metal matrix composites. *Journal of Materials Science*. 1998;33:3491–3503
- [10] Dobrzański LA, Kremzer M, Dziekońska M. Possibility of wettability improvement of Al₂O₃ preforms infiltrated by liquid aluminium alloy by deposition Ni-P coating. *Archives of Materials Science and Engineering*. 2012;55:14–21
- [11] Evans A, San Marchi C, Mortensen A. Metal matrix composites in industry: an introduction and a survey. New York: Springer Science+Business Media; 2003. 386 p.
- [12] Li RQ, Peng F, Guan JW, Yan XZ, Liu SZ, Zhang WK, Zhou XL. Pressure infiltration of boron nitride preforms with molten aluminum for low density heat sink materials. *Journal of Materials Science Materials in Electronics*. 2013;24:1175–1180. doi:10.1007/s10854-012-0901-8
- [13] Freitas M, Pianaro SA, Nadal FN, Tebcherani SM, Berg EAT. Preparation and characterization of SiC/kaolin/Al composite materials by squeeze-casting (in Portuguese). *Cerâmica*. 2009;55:271–280. doi:10.1590/S0366-69132009000300006
- [14] Tomiczek B, Kujawa M, Matula G, Kremzer M, Tański T, Dobrzański LA. Aluminium AlSi12 alloy matrix composites reinforced by mullite porous preforms. *Materials Science & Engineering Technology. Materialwissenschaft und Werkstofftechnik*. 2015;46:368–376. doi:10.1002/mawe.201500411
- [15] Dobrzański LA, Kremzer M, Gołombek K. Structure and properties of aluminum matrix composites reinforced by Al₂O₃ particles. *Materials Science Forum*. 2008;591–593:188–192
- [16] Kremzer M, Dobrzański LA, Dziekońska M, Radziszewska A. Structure and properties of aluminium-silicon matrix composites manufactured by pressure infiltration method. *Archives of Materials Science and Engineering*. 2014;68:53–58

- [17] Pawlyta M, Tomiczek B, Dobrzański LA, Kujawa M, Bierska-Piech B. Transmission electron microscopy observations on phase transformations during aluminium/mullite composites formation by gas pressure infiltration. *Materials Characterization*. 2016;114:9–17. doi:10.1016/j.matchar.2016.02.003
- [18] Tomiczek B, Pawlyta M, Adamiak M, Dobrzański LA. Effect of milling time on microstructure of AA6061 composites fabricated via mechanical alloying. *Archives of Metallurgy and Materials*. 2015;60:789–793. doi:10.1515/amm-2015-0208
- [19] Dobrzański LA, Tomiczek B, Matula G, Gołombek K. Role of halloysite nanoparticles and milling time on the synthesis of AA 6061 aluminium matrix composites. *Advanced Materials Research*. 2014;939:84–89
- [20] Dobrzański LA, Tomiczek B, Pawlyta M, Król M. Aluminium AlMg1SiCu matrix composite materials reinforced with halloysite particles. *Archives of Metallurgy and Materials*. 2014;59:335–338. doi:10.2478/amm-2014-0055
- [21] Dobrzański LA, Tomiczek B, Pawlyta M, Nuckowski P. TEM and XRD study of nanostructured composite materials reinforced with the halloysite particles. *Materials Science Forum*. 2014;783–786:1591–1596
- [22] Dobrzański LA, Tomiczek B, Pakieła W, Tomiczek AE. Mechanical properties and wear resistance of PM composite materials reinforced with the halloysite particles. *Advanced Materials Research*. 2015;1127:107–112
- [23] Dobrzański LA, Kremzer M, Nowak AJ, Nagel A. Aluminium matrix composites fabricated by infiltration method. *Archives of Materials Science and Engineering*. 2009;36:5–11
- [24] Kremzer M. Structure and properties of EN AC- AlSi12 alloy matrix composites manufactured by pressure infiltration method [Ph.D. Thesis]. Gliwice, Poland: Silesian University of Technology; 2007 (in Polish)
- [25] Dobrzański LA, Kremzer M, Nagel A. Structure and properties of ceramic preforms based on Al_2O_3 particles. *Journal of Achievements in Materials and Manufacturing Engineering*. 2009;35:7–13
- [26] Mizuuchi K, Takeuchi T, Inoue K, Lee JH, Sugioka M, Itami M, Kawahara M, Yamauchi I, Asanuma H. Properties of boron fiber reinforced aluminum matrix composites fabricated by pulsed current hot pressing (PCHP). *Materials Science Forum*. 2007:539–543:3139–3144
- [27] Luo Z, Song Y, Zhang S, Miller DJ. Interfacial microstructure in a $\text{B}_4\text{C}/\text{Al}$ composite fabricated by pressureless infiltration. *Metallurgical and Materials Transactions: A*. 2012;43:281–293. doi:10.1007/s11661-011-0817-6
- [28] Lee KB, Sim HS, Kwon H. Reaction products of Al/TiC composites fabricated by the pressureless infiltration technique. *Metallurgical and Materials Transactions: A*. 2005;36:2517–2527. doi:10.1007/s11661-006-0052-8

- [29] Adamiak M. The effect of TiAl and Ti₃Al reinforcement on microstructure changes and properties of aluminium matrix composites. *Archives of Materials Science and Engineering*. 2012;58:55–79
- [30] Dobrzański LA, Dobrzańska-Danikiewicz AD, Gaweł TG, Achteлик-Franczak A. Selective laser sintering and melting of pristine titanium and titanium Ti6Al4V alloy powders and selection of chemical environment for etching of such materials. *Archives of Metallurgy and Materials*. 2015;60:2039–2045. doi:10.1515/amm-2015-0346
- [31] Dobrzański LA, Dobrzańska-Danikiewicz AD, Malara P, Gaweł TG, Dobrzański LB, Achteлик-Franczak A. Fabrication of scaffolds from Ti6Al4V powders using the computer aided laser method. *Archives of Metallurgy and Materials*. 2015;60:1065–1070. doi:10.1515/amm-2015-0260
- [32] Dobrzański LA, Tomiczek B, Adamiak M. Manufacturing of EN AW6061 matrix composites reinforced by halloysite nanotubes. *Journal of Achievements in Materials and Manufacturing Engineering*. 2011;49:82–89
- [33] Zhang H, Maljkovic N, Mitchell BS. Structure and interfacial properties of nanocrystalline aluminum/mullite composites. *Materials Science and Engineering: A*. 2002;326:317–323. doi:10.1016/S0921-5093(01)01500-3
- [34] Dobrzański LA, Kremzer M, Nowak AJ, Nagel A. Composite materials based on porous ceramic preform infiltrated by aluminium alloy. *Journal of Achievements in Materials and Manufacturing Engineering*. 2007;20:95–98
- [35] Peng LM, Cao JW, Noda K, Han KS. Mechanical properties of ceramic-metal composites by pressure infiltration of metal into porous ceramics. *Materials Science and Engineering A*. 2004;374:1–9. doi:10.1016/j.msea.2003.12.027
- [36] Yuan P, Tan D, Annabi-Bergaya F. Properties and applications of halloysite nanotubes: recent research advances and future prospects. *Applied Clay Science*. 2015;112–113: 75–93
- [37] Garcia-Cordovilla C, Louis E, Narciso J. Pressure infiltration of packed ceramic particulates by liquid metals. *Acta Materialia*. 1999;47:4461–4479. doi:10.1016/S1359-6454(99)00318-3
- [38] Kang CG, Seo YH. The influence of fabrication parameters on the deformation behavior of the preform of metal-matrix composites during the squeeze-casting processes. *Journal of Materials Processing Technology*. 1996;61:241–249. doi:10.1016/0924-0136(95)02180-9
- [39] Yamauchi T, Nishida Y. Infiltration kinetics of fibrous preforms by aluminum with solidification. *Acta Metallurgica et Materialia*. 1995;43:1313–1321. doi:10.1016/0956-7151(94)00374-Q

- [40] Eardley ES, Flower HM. Infiltration and solidification of commercial purity aluminium matrix composites. *Materials Science and Engineering: A*. 2003;359:303–312. doi:10.1016/S0921-5093(03)00357-5
- [41] Lianxi H, Yiwen Y, Shoujing L, Xinying X. Investigation on the kinetics of infiltration of liquid aluminium into an alumina fibrous preform. *Journal of Materials Processing Technology*. 1999;94:227–230. doi:10.1016/S0924-0136(99)00099-0
- [42] Etter T, Papakyriacou M, Schultz P, Uggowitzer PJ. Physical properties of graphite/aluminium composites produced by gas pressure infiltration method. *Carbon*. 2003;41:1017–1024. doi:10.1016/S0008-6223(02)00448-7
- [43] Travitzky NA. Microstructure and mechanical properties of alumina copper composites fabricated by different infiltration techniques. *Materials Letters*. 1998;36:114–117. doi:10.1016/S0167-577X(98)00012-3
- [44] Dobrzański LA, Kremzer M, Nagel A. Aluminium EN AC- AlSi12 alloy matrix composite materials reinforced by Al_2O_3 porous preforms. *Archives of Material Science and Engineering*. 2007;28:593–596
- [45] Dobrzański LA, Kremzer M, Nagel A. Application of pressure infiltration to the manufacturing of aluminium matrix composite materials with different reinforcement shape. *Journal of Achievements in Materials and Manufacturing Engineering*. 2007;24:183–186
- [46] Mattern A, Huchler B, Stadenecker D, Oberacker R, Nagel A, Hoffmann MJ. Preparation of interpenetrating ceramic-metal composites. *Journal of European Ceramic Society*. 2004;24:3399–3408. doi:10.1016/j.jeurceramsoc.2003.10.030
- [47] Luo ZP, Song YG, Zhang SQ. A TEM study of the microstructure of SiC_p/Al composite prepared by pressureless infiltration method. *Scripta Materialia*. 2001;45:1183–1189. doi:10.1016/S1359-6462(01)01148-4
- [48] Ryu YM, Yoon EP, Rhee MH. The behavior of the nickel layer in an aluminum matrix composite reinforced with nickel coated carbon fiber. *Journal of Materials Science Letters*. 2000;19:1103–1105. doi:10.1023/A:1006780212533
- [49] Dobrzański LA, Tomiczek B, Adamiak M, Matula G, Sołtys J. Nanostructure composite material with wrought aluminum alloy and method for production thereof. Patent PL 216257. 2014
- [50] Dobrzański LA, Tomiczek B, Kremzer M, Matula G, Sołtys J. Composite material with casting aluminum alloys matrix and method for producing thereof. Patent PL 217093. 2014
- [51] León CA, Drew RAL. The influence of nickel coating on the wettability of aluminum on ceramics. *Composites A*. 2002;33:1429–1432. doi:10.1016/S1359-835X(02)00161-6

- [52] Sobczak N, Asthana R, Radziwiłł W, Nowak R, Kudyba A. The role of aluminum oxidation in the wetting-bonding relationship of Al/oxide couples. *Archives of Metallurgy and Materials*. 2007;52:55–65
- [53] Pech-Canul MI, Katz RN, Makhlof MM, Pickard S. The role of silicon in wetting and pressureless infiltration of SiC_p performs by aluminum alloys. *Journal of Materials Science*. 2000;35:2167–2173. doi:10.1016/S0924-0136(00)00664-6
- [54] Hashim J, Looney L, Hashmi MSJ. The enhancement of wettability of particles in cast aluminium matrix composites. *Journal of Materials Processing Technology*. 2001;119:329–335. doi:10.1016/S0924-0136(01)00919-0
- [55] Dobrzański LA, Kremzer M, Adamiak M. The influence of reinforcement shape on wear behaviour of aluminium matrix composite materials. *Journal of Achievements in Materials and Manufacturing Engineering*. 2010;42:26–32
- [56] Dobrzański LA, Kremzer M, Nagel A, Huchler B. Fabrication of ceramic preforms based on Al₂O₃ CL 2500 powder. *Journal of Achievements in Materials and Manufacturing Engineering* 2006;18:71–74
- [57] Miazga A, Konopka K, Gizowska M, Szafran M. Alumina matrix ceramic-nickel composites formed by gelcasting method. *Composites Theory and Practise*. 2012;12: 138–141
- [58] Dobrzański LA, Matula G. Powder injection molding: sinter-hardening. In: Colás R, Totten GE, editors. *Encyclopedia of iron, steel, and their alloys*. Boca Raton: CRC Press, Taylor & Francis Group; 2016; 14 p. ISBN: 978-1-4665-1104-0
- [59] Matula G. Gradient surface layers from tool cermets formed pressurelessly and sintered. *Open Access Library*. 2012;7:1–144 (in Polish)
- [60] Dobrzański LA, Matula G. Powder metallurgy fundamentals and sintered materials. *Open Access Library*. 2012;8:1–156 (in Polish)
- [61] Krzysteczko J. Structure and properties of aluminium alloy matrix composites manufactured by powder injection moulding method [Ph.D. Thesis in progress]. Gliwice, Poland: Silesian University of Technology; 2016 (in Polish)
- [62] Kujawa M. Infiltrated AlSi12 alloy matrix composites reinforced with sintered halloysite nanotubes [Ph.D. Thesis]. Gliwice, Poland: Silesian University of Technology; 2015 (in Polish)
- [63] Dobrzański LA, Tomiczek B, Adamiak M, Gołombek K. Mechanically milled aluminium matrix composites reinforced with halloysite nanotubes. *Journal of Achievements in Materials and Manufacturing Engineering*. 2012;55:654–660
- [64] Dobrzański LA, et al. Investigations of structure and properties of newly created porous biomimetic materials fabricated by selective laser sintering, BIOLASIN. Project UMO-2013/08/M/ST8/00818. Silesian University of Technology, Gliwice; 2013–2016

- [65] Ahtelik-Franczak A. Engineering composite materials the reinforcement with the microporous titanium selective laser sintered [Ph.D. Thesis]. Gliwice, Poland: Silesian University of Technology; 2016 (in Polish)
- [66] Dobrzański LB. Structure and properties of the engineering materials applied on the stomatognathic system prostheses manufactured with additive and loss-processing methods [Ph.D. Thesis in progress]. Cracow, Poland: AGH University of Science and Technology; 2016 (in Polish)
- [67] Dobrzański LA, Dobrzańska-Danikiewicz AD, Malara P, Gaweł TG, Dobrzański LB, Ahtelik A. Composite fabricated by computer-aided laser methods for craniofacial implants and its manufacturing method. Patent Application P 411689. 23.03.2015
- [68] Dobrzański LA, Dobrzańska-Danikiewicz AD, Malara P, Gaweł TG, Dobrzański LB, Ahtelik-Franczak A. Bone implant scaffold. Patent Application P 414424. 19.10.2015
- [69] Dobrzański LA, Dobrzańska-Danikiewicz AD, Malara P, Dobrzański LB, Ahtelik-Franczak A. Biological and engineering composites for regenerative medicine. Patent Application P 414723. 9.11.2015
- [70] Dobrzański LA, Dobrzańska-Danikiewicz AD, Malara P, Gaweł TG, Dobrzański LB, Ahtelik-Franczak A. Implant scaffold and a prosthesis of anatomical elements of a dental system and craniofacial bone. Patent Application P 414423. 19.10.2015
- [71] Boccaccini AR, Karapappas P, Marijuan JM, Kaya C. TiO₂ coatings on silicon carbide and carbon fibre substrates by electrophoretic deposition. *Journal of Materials Science*. 2004;39:851–859
- [72] Pipel E, Woltersdorf J, Dietrich D, Stockel S, Weise K, Marx G. CVD-coated boron nitride on continuous silicon carbide fibres: structure and nanocomposition. *Journal of the European Ceramic Society*. 2000;20:1837–1844
- [73] Kuiry SC, Wannaparhun S, Dahotre NB, Seal S. In-situ formation of Ni-alumina nanocomposite during laser processing. *Scripta Materialia*. 2004;50:1237–1240. doi:10.1016/j.scriptamat.2004.02.005
- [74] Kremzer M, Dobrzański LA, Dziekońska M, Macek M. Atomic layer deposition of TiO₂ onto porous biomaterials. *Archives of Materials Science and Engineering*. 2015;75:63–69
- [75] Saiz E, Tomsia AP, Loehman RE, Ewsuk K. Effects of composition and atmosphere on reactive metal penetration of aluminium in mulita. *Journal of the European Ceramic Society*. 1996;16:275–280. doi:10.1016/0955-2219(95)00156-5
- [76] Kim BM, Cho YK, Yoon SY, Stevens R, Park HC. Mullite whiskers derived from kaolin. *Ceramics International*. 2009;35:579–583. doi:10.1016/j.ceramint.2008.01.017
- [77] Rawtani D, Agrawal YK. Multifarious applications of halloysite nanotubes: a review. *Reviews on Advanced Materials Science*. 2012;30:282–295

- [78] Kamble R, Ghag M, Gaikawad S, Panda BK. Halloysite nanotubes and applications: a review. *Advanced Scientific Research*. 2012;3:25–29
- [79] Lvov Y, Aerov A, Fakhrullin RL. Clay nanotube encapsulation for functional biocomposites. *Advances in Colloid and Interface Science*. 2014;207:189–198. doi:10.1016/j.cis.2013.10.006
- [80] Qia R, Guo R, Zheng F, Liu H, Yu J, Shi X. Controlled release and antibacterial activity of antibiotic-loaded electrospun halloysite/poly(lactic-co-glycolic acid) composite nanofibers. *Colloids and Surfaces B: Biointerfaces*. 2013;110:148–155. doi:10.1016/j.colsurfb.2013.04.036
- [81] Jiang L, Zhang C, Liu M, Yang Z, Tjiu WW, Liu T. Simultaneous reinforcement and toughening of polyurethane composites with carbon nanotube/halloysite nanotube hybrids. *Composites Science and Technology* 2014;91:98–103. doi:10.1016/j.compscitech.2013.11.025
- [82] Stoch L, Waclawska I. Dehydroxylation of kaolinite group minerals. I. Kinetics of dehydroxylation of kaolinite and halloysite. *Journal of Thermal Analysis*. 1981;20:291–304. doi:10.1007/BF01912877
- [83] Papoulis D, Komarneni S, Panagiotaras D, Stathatos E, Christoforidis KC, Fernández-García M, Li H, Shu Y, Sato T, Katsuki H. Three-phase nanocomposites of two nanoclays and TiO₂: synthesis, characterization and photocatalytic activities. *Applied Catalysis B: Environmental*. 2014;147:526–533. doi:10.1016/j.apcatb.2013.09.025
- [84] Dobrzańska-Danikiewicz AD. Foresight of material surface engineering as a tool building a knowledge based economy. *Materials Science Forum*. 2012;706–709:2511–2516. doi:10.4028/www.scientific.net/MSF.706-709.2511.
- [85] Dobrzańska-Danikiewicz AD, Dobrzański LA, Sękala A. Results of Technology Foresight in the Surface Engineering Area. *Applied Mechanics and Materials*. 2014;657:916–920. doi:10.4028/www.scientific.net/AMM.657.916
- [86] Dobrzańska-Danikiewicz AD. The acceptance of the production orders for the realisation in the manufacturing assembly systems. *Journal of Materials Processing Technology* 2006;175 :123–132. doi:10.1016/j.jmatprotec.2005.04.001
- [87] Dobrzański LA. Applications of newly developed nanostructural and microporous materials in biomedical, tissue and mechanical engineering. *Archives of Materials Science and Engineering*. 2015;76:53–114
- [88] Dobrzański LA. Application of the additive manufacturing by selective laser sintering for constituting implantscaffolds and hybrid multilayer biological and engineering composite materials. Keynote lecture on International Conference on Processing & Manufacturing of Advanced Materials THERMEC'2016, Processing, Fabrication, Properties, Applications. Graz, Austria; 29.05.2016–3.06.2016

- [89] Dobrzański LA. Fabrication, structure and mechanical properties of laser sintered materials for medical applications. Invited lecture on XXV International Materials Research Congress. Cancun, Mexico; 14.08.2016–19.08.2016
- [90] Dobrzański LA. Metallic implants-scaffolds for dental and orthopaedic application. Invited lecture on 9th COLAOb – Latin American Congress on Artificial Organs and Biomaterials. Foz do Iguacu, Brazil; 24.08.2016–27.08.2016

IntechOpen

IntechOpen

